AD-A185 655 ENTROPIC ELASTIC PROCESSES IN PROTEIN MECHANISMS PART 1 1/1
ELASTIC STRUCTURE. (U) ALABAMA UNIV IN BIRMINGHAM LAB
OF MOLECULAR BIOPHYSICS D W URRY 1986 N00014-86-K-0402
UNCLASSIFIED F/G 6/11 NL

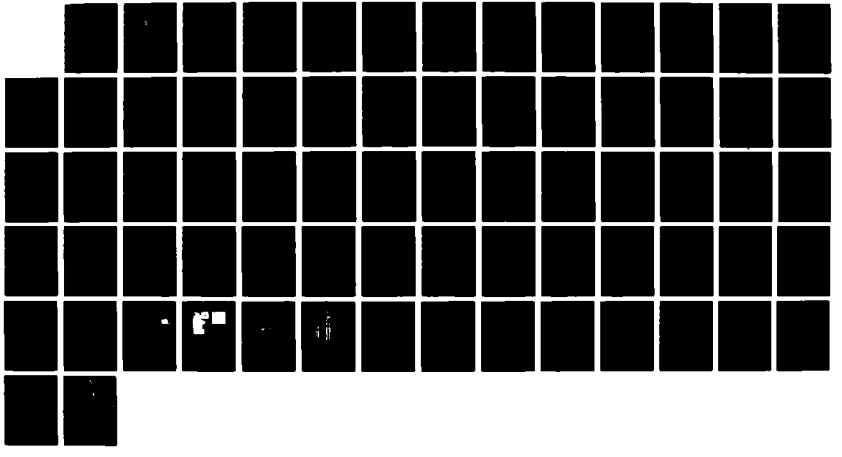

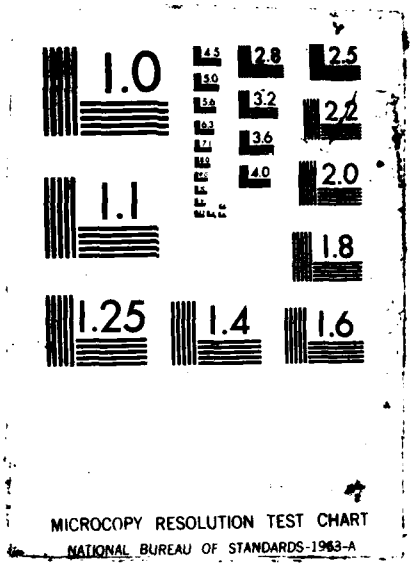
1.0
1.1
1.25
1.4
1.6
2.8
3.2
3.6
4.0
2.5
2.2
2.0
1.8
MICROCOPY RESOLUTION TEST CHART
NATIONAL BUREAU OF STANDARDS-1963-A

ENTROPIC ELASTIC PROCESSES IN PROTEIN MECHANISMS

PART 1. ELASTIC STRUCTURE DUE TO AN INVERSE TEMPERATURE TRANSITION AND ELASTICITY DUE TO INTERNAL CHAIN DYNAMICS

Dan W. Urry

Laboratory of Molecular Biophysics
The University of Alabama at Birmingham
P. O. Box 311/University Station
Birmingham, Alabama 35294

Contract N00014-86-K-0402

"At every crossway on the road that leads to the future,
tradition, has placed against each of us, 10,000 men to guard the pass."
Maurice Maeterlinck, 1907

ELASTIC PROCESSES IN PROTEIN MECHANISMS
PART 1. Elastic Structure due to an Inverse Temperature Transition and Elasticity due to Internal Chain Dynamics

Abstract:

Numerous physical characterizations clearly demonstrate that a polypentapeptide of elastin, $(Val^1\text{-}Pro^2\text{-}Gly^3\text{-}Val^4\text{-}Gly^5)_n$, in water undergoes an inverse temperature transition. Increase in order occurs both intermolecularly and intramolecularly on raising the temperature from 20° to 40°C. The physical characterizations utilized to demonstrate the inverse temperature transition include microscopy, light scattering, circular dichroism, the nuclear Overhauser effect, temperature dependence of composition, nuclear magnetic resonance relaxation, dielectric relaxation and temperature dependence of elastomer length. At fixed extension of the cross-linked polypentapeptide elastomer, development of elastomeric force is seen to correlate with increase in intramolecular order, that is, with the inverse temperature transition. Reversible thermal denaturation of the ordered polypentapeptide is observed with composition and circular dichroism studies, and thermal denaturation of the cross-linked elastomer is also observed with loss of elastomeric force and elastic modulus. Thus elastomeric force is lost when the polypeptide chains are randomized due to heating at high temperature. Clearly elastomeric force is due to non-random polypeptide structure. In spite of this, elastomeric force is demonstrated to be dominantly entropic in origin. The source of the entropic elastomeric force is demonstrated to be the result of internal chain dynamics and the mechanism is called the librational entropy mechanism of elasticity.

There is significant application to the finding that elastomeric force develops due to an inverse temperature transition. By changing the hydrophobicity of the polypeptide, the temperature range for the inverse temperature transition can be changed in a predictable way and the temperature range for the development of elastomeric force follows. Thus elastomers have been prepared where the development of elastomeric force is shifted over a 40°C temperature

range from a midpoint temperature of 30°C for the polypentapeptide to 10°C by increasing hydrophobicity with addition of a single CH_2 moiety per pentamer and to 50°C by decreasing hydrophobicity.

The implications of these findings to elastic processes in protein mechanisms are several: i. When elastic processes are observed in proteins, it is not necessary, and it may be incorrect, to attempt description in terms of random chain networks and random coils. ii. Rather than requiring a random chain network characterized by a random distribution of end-to-end chain lengths, entropic elastomeric force can be exhibited by a single, short peptide segment. iii. Perhaps of greatest significance whether occurring in a short peptide segment or in a fibrillar protein, it should be possible reversibly to turn "on" and "off" elastomeric force by reversibly changing the hydrophobicity of the polypeptide. Phosphorylation and dephosphorylation would be the most obvious means of changing the hydrophobicity of a polypeptide. These considerations are treated in the second paper, PART 2: Simple (Passive) and Coupled (Active) Development of Elastic Forces.

I. INTRODUCTION

It is the purpose of this the first of two articles to provide clarification of the basis of polypeptide entropic elastomeric force, its definition, the experimental basis for its identification, and, importantly, the source of entropy change on deformation. The nature of entropic elastomeric force will be demonstrated with the polypentapeptide of elastin, $(Val^1\text{-}Pro^2\text{-}Gly^3\text{-}Val^4\text{-}Gly^5)_n$, with the emergence of a new mechanism for the elasticity.[1] Entropic elasticity of this and related sequential polypeptides derives from regular spiral structures in which internal chain dynamics (librational motion) provides the entropic elastomeric force. The central point derived from studies on the polypentapeptide and its analogs is that entropic protein and polypeptide elasticity can be exhibited by regular, non-random conformations which can be denatured at temperatures greater than 60°C with loss of elastic force and loss of elastic modulus. Polypeptide elasticity does not require random coils or networks of random chains. In point of fact, thermally denatured polypeptide elastomers, i.e., the randomized polypeptide structures with no change in the number of cross-links, exhibit greatly reduced elastic moduli.

The specific case demonstrated is one in which entropic elastic states of polypeptides are obtained on the more ordered side of an inverse temperature transition. Since the temperature of the inverse temperature transition depends on the hydrophobicity of the polypeptide chain, it becomes apparent at a given temperature that elastomeric force can be turned "on" and "off" by changing the hydrophobicity of the polypeptide chain. Examples of chemical processes whereby the hydrophobicity of the polypeptide chain could be reversibly changed, i.e.,

[1] Presumably because of the firmly held view that the elasticity of elastin derived from random chain networks, the only published physical characterizations of the elastomeric sequential polypeptides of elastin are due to the work of this Laboratory. Because of this, the relevant work reviewed here, going back a decade and one-half, will require that an uncommon proportion of the refererces be to our own publications.

whereby the temperature of the transition could be reversibly shifted, are ionization/deionization as in the titration of a weak acid or base, enzymatic amidation/deamidation of carboxylates, and phosphorylation/dephosphorylation. The second article (PART 2) will consider the application of these concepts to entropic elastic processes of additional polypeptide and protein systems.

II. ENTROPIC ELASTOMERIC FORCE

A. Definition of Entropic Elastomeric Force

A material displays elastomeric force, f, when it resists and recovers from deformation. The elastomeric force is defined as the change in maximum work function (Helmholtz free energy), ∂A, with change in length, ∂L, at constant volume, V, and constant temperature, T, that is,

$$f \equiv \left(\frac{\partial A}{\partial L}\right)_{V,T} \tag{1}$$

But since

$$\left(\frac{\partial A}{\partial L}\right)_{V,T} = \left(\frac{\partial E}{\partial L}\right)_{V,T} - T\left(\frac{\partial S}{\partial L}\right)_{V,T} \tag{2}$$

where E is the internal energy and S is the entropy of the elastomeric system, the elastomeric force is described as having two components, an internal energy component, f_e, and an entropy component, f_s, i.e.,

$$f = f_e + f_s \tag{3}$$

On deformation, f_e is due to the strain in bonds and f_s, the entropic elastomeric force, results from a decrease in the number of configurations in the lowest energy band of states. Since bond strain leads to bond breakage, a durable, i.e., an ideal elastomer, would be one in which $f_e = 0$ and $f = f_s$. Elastin, the elastic protein of connective tissue, presents an extreme example of a durable

elastomer. Single elastic fibers can last the lifetime of an individual (Partridge, 1962; Sandberg, et al., 1977). Within the normal lifetime of the individual, single elastic fibers will have undergone a billion stretch-relaxation cycles in the aortic arch and thoracic aorta, where there is twice as much elastin as collagen (Cleary and Moont, 1977). Clearly one anticipates that this is a near ideal elastomer, that elastin exhibits a dominantly entropic elastomeric force. Obviously to be able to exert an elastomeric force without paying an internal energy price to do so would be a very useful mechanism in protein function. Just as apparent, an f_s in an elastomeric polypeptide segment should be usable to effect an f_e in an appropriately associated bond system. In particular, for it to be possible to use entropic elastomeric force to induce strain, that is to achieve an f_e, in a bond undergoing hydrolytic cleavage would be an effective means of reducing the internal energy barrier for a reaction and to increase the catalytic rate. But before such considerations have validity, it is necessary both to have means of identifying entropic elastomeric force and to understand the mechanism whereby entropic elastomeric force develops. For in the above example of strain in enzyme catalysis it was assumed that a single, short, anisotropic polypeptide chain segment, rather than an isotropic random network of chains, would be sufficient to exert an entropic elastomeric force.

B. Experimental Bases for Identifying Entropic Elastomeric Force

A means of evaluating the magnitude of the elastomeric force, f_s, is in experimentally determining the f_e/f ratio. Following Flory and colleagues (Flory et al., 1960; Andrady and Mark, 1980; Queslel and Mark, 1986).

$$\frac{f_e}{f} = -T\left(\frac{\partial \ln[f/T]}{\partial T}\right)_{V,L,n} \tag{4}$$

Accordingly the experiment is to stretch the sample to a fixed length, L, and for conditions of constant volume, V, and constant composition, n, to determine

the temperature dependence of force. The f_e/f ratio is obtained from a plot of $\ln(f/T)$ versus temperature where the slope times the mean of the absolute temperature for the temperature interval of interest is the f_e/f ratio. For a dominantly entropic elastomer f_e/f is less than 0.5. Two complications with the approach are that it is not common to be able to hold V and n constant with varying temperature and that T is large, usually greater than 300°K, requiring that the slope be determined very accurately. To overcome the former complication, an approximate correction term has been developed for conditions of constant pressure, P, constant length and for an elastomer in equilibrium, eq, with a solvent. The expression becomes (Dorrington and McCrum, 1977)

$$\frac{f_e}{f} = -T\left(\frac{\partial \ln[f/T]}{\partial T}\right)_{P,L,eq} - \frac{\beta_{eq}\, T}{\alpha^3\,(V_i/V) - 1} \qquad (5)$$

where $\beta_{eq} = (\partial \ln V/\partial T)_{P,L,eq}$ is the thermal expansion coefficient; α is the fractional increase in length, L/L_i where L_i is the initial length and L the length at fixed extension, and V_i and V are the volumes of the elastomer before and after elongation. This correction term is an approximation for an isotropic network of chains with a Gaussian distribution of end-to-end lengths. As seen below, the polypentapeptide of elastin is not isotropic and would not have a broad Gaussian distribution of end-to-end chain lengths. Fortunately as will also be seen below, in the temperature range from 40° to 60°C, the volume of the non-extended state and the composition are nearly constant such that Equation 4 can be considered.

Because of the limitations of Equations 4 and 5, it is useful to have additional means of evaluating the entropic nature of a polypeptide. In order for a polypeptide to exhibit entropic elastomeric force, the backbone must be able to undergo substantial motion and the states represented by the motion must be obtainable with only low energy barriers for going from one state to another.

Considering this, the temperature dependence of the backbone motion, e.g., of the correlation time for the motion, can be determined. If the energy of activation for the motion is several kcal/mole or higher, then the states could not be sufficiently interconverting at body temperature to give a large entropy to the backbone. If on the other hand the activation energy is low, e.g., less than 2 kcal/mole, then the states would be reasonably obtainable at body temperature and the polypeptide backbone would have high entropy. The temperature dependence of backbone correlation time can be obtained from nuclear magnetic resonance and dielectric relaxation studies.

C. Proposed Mechanisms of Entropic Protein Elasticity

Having defined and arrived at means for identifying entropic elastomeric force (EEF), it is necessary to develop an understanding of the mechanism as this determines the potential for EEF to be a factor in protein mechanisms.

1. Classical Theory of Rubber Elasticity: Decrease in entropy on deformation due to displacement from random distribution of end-to-end chain lengths

In the classical theory of rubber elasticity, the description is one of a random chain network in which there is a random distribution of end-to-end chain lengths (Flory, 1953; Mandelkern, 1983). This is shown in Figure 1 where the probability of a given end-to-end chain length, W(r), is plotted against the value of the end-to-end chain length for a freely jointed chain comprised of 10,000 units with a repeat length of 0.25 nm (Queslel and Mark, 1986; Flory, 1953). The end-to-end chain lengths vary from 0 nm to fully extended with a peaking near 20 nm. A random chain network is an isotropic system. One random chain configuration with the end-to-end chain length indicated as r is given in Figure 2 (Flory, 1953). A collection of such chains with a random distribution of end-to-end chain lengths is what is represented by the solid

curve in Figure 1. As developed by Flory and coworkers (Flory, et al., 1960), calculation of the f_e/f ratio is achieved by the expression

$$\frac{f_e}{f} = -T\left(\frac{d \ln \langle r^2 \rangle_o}{dT}\right) \quad (6)$$

where $\langle r^2 \rangle_o$ is the mean square end-to-end chain length calculated beginning with the equation of Eyring (Eyring, 1932). That the elasticity of elastin is due to random chain networks is a staunchly held view (Hoeve and Flory, 1958 and 1974; Aaron and Gosline, 1980 and 1981; Torchia, et al., 1983; Torchia and Piez, 1973; Lyerla and Torchia, 1975; Gosline and Rosenbloom, 1984; Andrady and Mark, 1980; Flemming, et al., 1980).

2. Solvent Entropy: Decrease in entropy on deformation due to exposure of hydrophobic side chains that become surrounded by clathrate-like water of lower entropy than bulk water

The amino acid composition of mammalian elastin, for example, is one of 60% hydrophobic residues, one-third glycine residues and the remainder largely due to lysine residues that become cross-links with loss of charge (Petruska and Sandberg, 1968; Franzblau and Lent, 1969). Thus in terms of amino acid composition, elastin is a hydrophobic protein. On stretching of elastin, it is to be expected that hydrophobic association of side chains will become disrupted and that less-ordered bulk water will surround the exposed hydrophobic side chains and become more-ordered clathrate-like water. Thus a decrease in solvent entropy is expected on extension of elastin and this has been proposed to contribute to entropic elastomeric force (Weis-Fogh and Andersen, 1970; Gosline, 1978 and 1980; Gray, et al., 1973).

3. Librational Entropy Mechanism of Elasticity: Decrease in entropy on deformation due to damping of internal chain dynamics

The librational entropy mechanism of elasticity was derived from

studies on the conformation and function of the polypentapeptide of elastin (Urry, 1982; Urry, et al., 1982; Urry and Venkatachalam, 1983; Urry, et al., 1985f).[2] The mechanism, however, is entirely general. In the non-stretched state, a polypeptide chain segment is able to exhibit internal chain dynamics involving large amplitude, low frequency rocking motions of composite moieties, the simplest of which would be the peptide moiety. On stretching the amplitude of the rocking motions (of the librations) is damped and may be shifted to higher frequency. This constitutes a decrease in entropy of the chain segment.

In its range of expressions of elastic force, the librational entropy mechanism (LEM) may involve only a small chain segment comprised of but a few residues. Alternatively the LEM may involve a regular dynamic structure. The regular elastic structure, for example comprised of repeating peptide sequences, is intermediate in its entropic state between the more rigid α-helix, β-sheets and triple-stranded collagen structures at the one extreme and the classically considered random chain network (random coil structure) at the other extreme. An example of such a regular structure is the polypentapeptide of elastin, $(Val^1\text{-}Pro^2\text{-}Gly^3\text{-}Val^4\text{-}Gly^5)_n$. Stages in the development of the conformation of the polypentapeptide of elastin have been reviewed elsewhere (Urry and Long, 1976; Urry, 1982, 1984). Here one member of the class of conformations is demonstrated in the relaxed and extended states. The molecular conformation of a relaxed β-spiral of the polypentapeptide is shown in Figure 3 (Venkatachalam and Urry, 1981; Urry, 1983; Urry, et al., 1982; Cook, et al., 1980). A spiral is defined as the helical recurrence of a repeating conformational feature (Urry, 1972 and 1974). The prefix β- signifies that the β-turn (see

[2] The polypentapeptide of elastin $(VPGVG)_n$ recurs eleven plus times in porcine and bovine elastin (Sandberg, et al., 1981; Rosenbloom, private communication), it forms the longest sequence between cross-links, and it is centrally located in the sequence (Rosenbloom, private communication, see Figure 1 of PART 2.)

Figure 3A) is the dominant secondary structural feature in the spiral. The β-spiral of the polypentapeptide of elastin is a helical structure (see Figures 3B and C) resulting from an inverse temperature transition in which intramolecular hydrophobic contacts are optimized. The β-turns function as spacers between turns of the spiral and between the β-turns are suspended segments within which large amplitude, low frequency librations can occur. In Figure 4A, a pentadecapeptide is shown in which a central pentamer has been allowed to undergo rocking motions (librations) the amplitudes of which are within an energy cut-off of 2 kcal/mole residue (Urry and Venkatachalam, 1983). On extension along the β-spiral axis to a length of 130% in Figure 4B, the amplitudes of the librations within the central pentamer for the same cut-off energy are seen to have become markedly damped. This decrease in amplitude of the librations on extension constitutes a large decrease in the entropy of the pentapeptide segment. The decrease in entropy provides resistance to extension and the increase in entropy on return to the relaxed (non-stretched) state constitutes the driving force for recovery from deformation. This is called the librational entropy mechanism of elasticity and the resulting entropic elastomeric force can occur within a single short peptide segment or within a regular spiral structure.

III. DEVELOPMENT OF STRUCTURE AND ENTROPIC ELASTOMERIC FORCE DUE TO AN INVERSE TEMPERATURE TRANSITION

A. Definition of an Inverse Temperature Transition

One statement of the second law of thermodynamics is that entropy of a total system of constant composition must increase with increase in temperature. When the system is multicomponent and one component within the total system undergoes a decrease in entropy with increase in temperature, that component is said to have undergone an inverse temperature transition. When the total system

is the two-component polypeptide-plus-water system and the polypeptide exhibits the inverse temperature transition, then the water component must have undergone an even greater increase in entropy through the temperature range of the inverse temperature transition in order that the total system will have experienced an increase in entropy on passing through the temperature range of note. This is understood by realizing that, below the transition, water surrounding hydrophobic side chains is more-ordered than bulk water (Frank and Evans, 1945; Kauzmann, 1959; Tanford, 1973). This more-ordered water is called clathrate-like water which is thought to be characterized by a hydrogen-bonding network referred to as a pentagonal dodecahedron (Swaminathan, et al., 1978). On raising the temperature through the transition range, the clathrate-like water becomes less-ordered bulk water as the hydrophobic side chains associate increasing the order in the polypeptide. With polymers of the repeat peptides of elastin, the increase in order of the polypeptide part of the system with increase in temperature has been demonstrated in numerous ways: by light and electron microscopy, by circular dichroism, by dielectric relaxation, by nuclear magnetic resonance and by the nuclear Overhauser effect which provided direct observation of hydrophobic side chain associations attending the inverse temperature transition. Also there is evidence in the same system using dielectric relaxation that the amount of clathrate-like water decreases rapidly with increase in temperature through the same temperature range as the order in the polypeptide increases (Buchet, et al., submitted).

B. Coacervation of the Polypentapeptide (Fibrillogenesis)

1. Definition of Coacervation

The polypentapeptide of elastin, abbreviated PPP, is soluble in water below 25°C. On raising the temperature above 25°C, aggregation occurs. Shown in Figure 5 are curves of the development of turbidity at 300 nm for dif-

ferent concentrations. The development is seen to be concentration dependent in an interesting way. On raising the concentration, the temperature profile for turbidity formation shifts to lower temperature and becomes steeper until a high concentration limit is reached, a limit which depends on molecular weight (Urry, et al., 1985e). When the turbid solution is allowed to stand, the more dense aggregates settle. When the process is reversible and the more dense phase is viscoelastic and of fixed composition as it is for the polypentapeptide in water, the process is called coacervation (Bungenberg de Jong and Kruyt, 1929, 1930 and 1949) and the more dense phase is called the coacervate. The overlying solution is called an equilibrium solution and the concentration of PPP in the equilibrium solution decreases as the molecular weight of the PPP is increased. The curves in Figure 5 then can be called temperature profiles for coacervation (Urry, et al., 1985e).

2. *Development* of the Phase Diagram

The temperature dependence of the composition of the PPP-plus-water system is shown in Figure 6 (Urry, et al., 1985e; Urry, in press). At 20°C, the polypentapeptide and water are miscible in all proportions. On raising the temperature to 30°C when there is more than 63% water by weight, there is a phase separation (coacervation occurs) with the development of an overlying equilibrium solution. At this temperature, the equilibrium solution is removed and the tube is resealed. The 30°C composition of the coacervate is 37% peptide and 63% water by weight. Continuing to raise the temperature to 60°C shows only a small expression of an overlying equilibrium solution such that at 60°C the composition is 38% peptide and 62% water by weight. In the temperature interval of 40° to 60°C, the coefficient of thermal expansion, $\beta_{eq} = (\partial \ln V/\partial T)$, is 2.4×10^{-4}/ deg. Very interestingly above 60°C there is a dramatic expulsion of water reaching at 80°C a composition of 68% peptide and 32%

water by weight. The entire process is reversible. With the data in Figure 6, a phase diagram can be constucted as shown in Figure 7 which also includes information on associated polypeptide structural transitions (Urry, et al., 1985e; Urry, 1985).

3. Fibrillogenesis

As shown in Figure 8, the process of coacervation is also a process of fibrillogenesis. The polypentapeptide of elastin self-assembles to form fibers. As seen in the scanning electron micrograph of Figure 8B, a single fiber is seen to splay-out into many parallel aligned fibrils and to recoalesce to form the same-sized fiber (Urry, et al., 1976). In Figure 8A, a transmission electron micrograph with negative staining shows a fibril to be comprised of parallel aligned filaments with a filament width of about 5nm (Volpin, et al., 1976). As will be shown below and as also follows from Figure 3, there is intramolecular ordering during coacervation which provides the β-spirals which associate to form the filaments for the intermolecular ordering of Figure 8, and the expulsion of water above 60°C, seen in Figure 6, is the denaturation of the ordered polypentapeptide as would occur with the loss of the intraspiral water within the structure shown in Figure 3D and E.

C. Correlation of Structure Development with Elastomeric Force Development

1. Formation of Polypentapeptide Elastomers

When a tube as in Figure 6 containing coacervate at a composition of about 38% peptide and 62% water by weight is γ-irradiation cross-linked with a 20×10^6 radiation absorbed dose (20 MRAD), a cylindrical elastomeric matrix is produced (see Figure 9A) (Urry, et al., 1986d). By nuclear magnetic resonance analysis, there is little or no detectable change in the carbon-13 and nitrogen-15 NMR spectra (even with 90%+ enrichment) resulting from the γ-irradiation, and a longitudinal relaxation rate study as a function of temperature demonstrates a

transition to decreased mobility on going from 25° to 40°C that is essentially the same for coacervate as for elastomer, i.e. 20 MRAD cross-linked coacervate (see Figure 9C) (Urry, et al., 1986d; Urry, et al., 1985d). With the cylindrical shape, the cross-sectional area can be accurately determined and the initial elastic modulus is found to be 1×10^6 dynes/cm^2. Also the change in volume on extension is easily determined with the cylindrical elastomer such that the V_i/V ratio of Eq. 5 is known. This NMR study demonstrates in the coacervate and in the elastomer a new characterization of an inverse temperature transition to be a decrease in backbone mobility with increasing temperature at constant composition; it also demonstrates the equivalence of the coacervate and γ-irradiation cross-linked elastomeric states.

For a more practical shape for mechanical characterizations in the studies noted below, the coacervate is formed in the bottom of a cryotube and a pestle containing a channel is inserted into the tube (Urry and Prasad, 1985). The coacervate flows into the circular channel. On γ-irradiation, circular elastomeric bands are formed of whatever desired dimensions. Commonly the channel is cut about 0.7 mm deep and 7 mm wide and a tube size is commonly chosen which gives a band of about 30 mm in circumference before cutting. A resulting elastomeric band is shown in Figure 9D along with the tube and pestle (Figure 9E).

2. Demonstration of Entropic Elastomeric Force

Following Equations 4 and 5, a small strip of the synthetic elastomeric band of Figure 9D is placed in a pair of grips and stretched to a fixed extension while immersed in water. The force is then monitored as a function of temperature and the resulting data is plotted in Figure 10 as f/T(°K) versus temperature; when plotted as ln[f/T(°K)] versus temperature following Equations 4 and 5, above 40°C there is a near zero slope (-4.5×10^{-4}/deg). Because of the equivalence of the coacervate and the synthetic elastomeric band of PPP, the

value of β_{eq} in Eq. 5 can be determined from the data in Figure 6 to be 2.4 x 10^{-4}/deg and using a value for the volume ratio, V_j/V, determined from stretching the cylinder (Figure 9B) to the 63% extension, the calculated f_e/f ratio for the data in Figure 10 in the temperature interval of 40° to 65°C is 0.12. The result is consistent in this temperature range with the PPP being dominantly an entropic elastomer. There are problems, however, with using the second term on the right-hand side of Eq. 5; an isotropic network of chains with a Gaussian distribution of end-to-end lengths has been assumed to make this correction, whereas the data in Figure 8 demonstrate an anisotropic fibrillar system at the molecular level. This situation is aided somewhat by the near constant volume and composition demonstrated in Figure 6 for the 40° to 60°C temperature range such that Eq. 4 is approximately correct; from Eq. 4 the f_e/f ratio would be 0.15. There is however the added complication that the near zero slope of Figure 10 may be due to the development of elastomeric force resulting from the inverse temperature transition in the 20° to 40°C temperature range and a decrease in elastomeric force above 60°C due to thermal denaturation (see Figure 16 below).

Another measure of the entropic nature of the elastomeric force can be the determination of the temperature dependence of the backbone motions. The requisite data is in Figure 9C. Above 40°C there is a linear increase in mobility with increase in temperature plotted as the inverse of the absolute temperature T^{-1} (°K). From the plot for both the coacervate and the cylindrical elastomer, the energy barrier for backbone mobility is approximately 1.5 kcal/mole (Urry, et al., 1986d). This indicates that backbone motion occurs with a sufficiently low energy of activation that a large number of states can be achieved at physiological temperatures as required of an entropic elastomer. This is further demonstrated by the large amplitude, low frequency backbone

librations observed in the dielectric relaxation data (see Figure 12 below). Thus, it is concluded that the polypentapeptide of elastin exhibits a dominantly entropic elastomeric force.

3. Correlations of Inverse Temperature Transition (Structure Development) with Development of Force at Fixed Extension

In Figure 10, there is a dramatic increase of elastomeric force between 20° and 40°C demonstrated for an elastomer that had been stretched 63% at 40°C. This development of elastomeric force correlates with a structural transition, many different facets of which have been observed by a range of different physical characterizations (Urry, 1984, 1985; Urry, et al., in press; Urry, et al., 1985b). The physical characterizations range from the macroscopic where the unaided eye is the analytical tool, to the microscopic, to the molecular and to the atomic levels of characterization. The sum of the results leave no question but that the molecular basis for the development of entropic elastomeric force is internal dynamics within a regular, non-random structure. It is that the elasticity being examined is due to a sequential polypeptide, namely the polypentapeptide of elastin, that allows the demonstration and conclusion of a new molecular basis for entropic elastomeric force to be so uncomprised. In what follows is a brief listing of some of the telling characterizations.

a. Temperature Profiles for Coacervation: In Figure 5, it is seen that clear solutions of polypentapeptide (PPP) in water become cloudy as the temperature is raised above 25°C. The onset of aggregation (turbidity) correlates closely with the rise in elastomeric force seen in Figure 10.

b. Microscopy: When a droplet of cloudy solution of Figure 5 is placed on a carbon coated grid, negatively stained with uranyl acetate and oxalic acid at pH 6.2, and examined in the transmission electron microscope, the filamentous aggregates of Figure 8A are observed. Optical diffraction of the

micrographs demonstrate periodicities, most prominently a 5 nm lateral spacing of the filaments and also an off-meridional reflection indicating an underlying helicity to the filaments (Volpin, et al., 1976). When two syntheses of the PPP are carried out, one having an occasional Glu residue in position four and the second having an occasional Lys residue in position four, and when solutions of the two syntheses are combined and a water soluble carbodiimide coupling reagent is added during aggregation, cross-linking occurs and the molecular system is seen to have self-assembled into fibers. This can be observed with a light microscope with no fixative (Urry, 1983) and in the scanning electron microscope with an aluminum coating as shown in Figure 8B (Urry, et al., 1976). Accordingly, during the development of elastomeric force in the 20° to 40°C temperature range, at the molecular level there is a self-assembly to form fibrillar structures.

c. Circular Dichroism Studies: When a series of circular dichroism (CD) curves are obtained at different temperatures on a 2.3 mg/ml solution of PPP in water and the ellipticity at 197 nm is plotted as a function of temperature on the left-hand ordinate and the elastomeric force of 20 MRAD cross-linked PPP coacervate at 60% extension is plotted on the right-hand ordinate as in Figure 11, the two curves are found to coincide (Urry, et al., 1985c). The complete CD spectrum below 25°C is more nearly that of a disordered polypeptide whereas the CD spectrum at elevated temperatures is characteristic of a polypeptide containing recurring Type II β-turns (see Figure 3A for the β-turn and Figure 15 below for the complete CD spectra). Thus intramolecular order increases as elastomeric force develops.

d. Nuclear Overhauser Effect Studies: Specific intramolecular hydrophobic side chain associations attending the inverse temperature transition of the elastomeric des Val^4 analog of the PPP of elastin (Urry, et al.,

1977) as well as for the PPP itself, (Khaled and Urry, unpublished data) have been determined by means of nuclear Overhauser enhancement studies. On raising the temperature into the range of the inverse temperature transition, there develops a close proximity of the $Val^1\gamma\underline{CH_3}$ moieties with the $Pro^2\delta\underline{CH_2}$ moieties. This identifies an intrapentamer part of the intramolecular hydrophobic association responsible for the inverse temperature transition. Evidence has most recently been obtained for $Val\gamma\underline{CH_3}$ - $Pro\beta\underline{CH_2}$ interturn, intramolecular hydrophobic interactions (Urry, et al., in preparation, a).

e. Composition Studies: In Figure 6, there is observed a phase transition which occurs in the same temperature interval in which elastomeric force develops in Figure 10. The composition of the coacervate as noted above at 40°C is 38% peptide and 62% water by weight (Urry, et al., 1985e). This coacervate composition was used in the nuclear magnetic resonance and dielectric relaxation studies noted below.

f. Nuclear Magnetic Resonance Relaxation Studies: When nuclear magnetic resonance relaxation studies are carried out on the coacervate phase at the 40°C composition (Urry, et al., 1985d) and on the cylindrical elastomer (Urry, et al., 1986d) as shown in Figures 9A, B and C, the polypeptide backbone mobility increases on raising the temperature to near 20°C. Above 20°C there occurs a marked decrease in mobility, without any change in water content, until the inverse temperature transition is over near 40°C. Above 40°C, the usual increase in mobility with increase in temperature resumes. Since temperature is the measure of molecular motion, this inverse behavior of decrease in backbone motion with increase in temperature provides a new definition of an inverse temperature transition. Again, it is during this inverse behavior that elastomeric force develops.

g. Dielectric Relaxation Studies: In the polypentapeptide-plus-water system, the only dipole moments are those of the water molecules and those of the peptide moieties of the polypeptide backbone. Accordingly, a relaxation that develops with its frequency above 10 MHz with a low energy of activation is clearly due to the polypentapeptide backbone motion. When the real part of the dielectric permittivity at 3.9 MHz divided by the temperature (°K) is plotted for the 40°C coacervate composition as a function of temperature as shown on the right-hand side of Figure 10, the development of relaxation intensity corresponds with the development of elastomeric force (Urry, et al., 1984). The real part of the dielectric permittivity is plotted in Figure 12A for the 1 MHz to 1 GHz frequency range for a series of temperatures through the transition (Henze and Urry, unpublished data). The relaxation is seen to occur with a localized frequency as is most clearly shown in Figure 12B where the 40°C minus 20°C difference curve is plotted from the data of Henze and Urry (1985). The difference curve is seen to be a nearly ideal Debye-type relaxation. This requires that the peptide dipole moments responsible for the relaxation are all oscillating at the same frequency. Because the energetics for peptide rocking motions would be different for pentamers in different conformations, or in a random chain network (Lyerla and Torchia, 1975), the common frequency requires that each pentamer during the transition comes into the same conformation, that is, a regular non-random conformation develops during the transition (Henze and Urry, 1985). Again, the development of elastomeric force is seen to correspond with the development of a regular structure, i.e. with an increase in intramolecular order.

h. Temperature Dependence of Elastomer Length: A strip of elastomeric PPP is equilibrated at 40°C and stretched to 60% and the force so-developed is then maintained as the temperature is varied. Like all entropic elastomers, as the temperature is raised, the elastomer shortens. The inter-

ting feature about the elastomeric PPP is that the length change is exaggerated in the 20° to 40°C temperature (Urry, et al., 1986b). Whereas latex will shorten less than 10% from 100% at 20°C to 90% plus at 40°C, the elastomeric polypentapeptide shortens by 30%, from 100% at 20°C to near 70% at 40°C. This differential behavior is even more dramatic in the absence of a load. Latex will expand by about 5% on going from 20°C to 40°C in the absence of a load. The elastomeric polypentapeptide on going from 20°C to 40°C undergoes a remarkable shortening from 100% at 20°C to near 40% at 40°C as shown in Figure 13. This dramatic shortening is the result of structure formation, i.e., of the winding up into a helical structure. Interestingly the change in length is approximately what is to be expected if the β-spiral of Figure 3 simply unwound with retention of β-turns (Thomas, et al., in press). Thus the development of elastomeric force in Figures 10 and 11 is due in part to the shortening of end-to-end chain length when the β-spiral structure forms as the result of the inverse temperature transition.

D. Application of the Principle that Elastomeric Force Develops as the Result of an Inverse Temperature Transition

It has been established repeatedly above that at fixed length, elastomeric force develops as the result of an inverse temperature transition. In general, the temperature range in which an inverse temperature transition occurs varies inversely with the hydrophobicity of the polypeptide chain. Accordingly, the correlation established above should be useful to change the temperature at which the development of elastomeric force occurs. This can be done by the replacement of a valyl residue with a more hydrophobic isoleucyl residue. This simple addition of a CH_2 moiety has no effect on the conformation of the polypentapeptide (Urry, et al., 1986c); yet as shown in Figure 14A, the temperature profiles of coacervation are shifted to lower temperatures. In Figure 14B, the

increase in intramolecular order with increase in temperature as followed by circular dichroism is shifted to lower temperatures. And very significantly as shown in Figure 14C, the development of elastomeric force has shifted from a midpoint near 30°C for the PPP of elastin to a midpoint near 10°C for the Ile^{1}-PPP elastomer (Urry, et al., 1986c).

By decreasing the hydrophobicity (increasing the hydrophilicity) of the polypeptide, the temperature of the transition can be raised. This is achieved with the des Val^{4}-PPP, that is, with the polytetrapeptide $(Val^{1}\text{-}Pro^{2}\text{-}Gly^{3}\text{-}Gly^{4})_{n}$. In Figure 14A, the temperature profiles for coacervation are seen to be shifted to higher temperature as is the development of intramolecular order (see Figure 14B). And as is expected, the development of elastomeric force has also been shifted to higher temperatures to a midpoint for the transition of near 50°C, some 20°C higher than for the PPP (Urry, et al., 1986a). Thus there is established the fundamental point that the temperature range for the development of elastomeric force can be shifted by changing the hydrophobicity or hydrophilicity of the elastomeric polypeptide. This can be expected to be of significance in protein mechanisms (see PART 2, the second article in this series).

E. Thermal Denaturation

It has been established that the elastomeric state of the PPP of elastin is one of a non-random regular structure. The proposed class of conformations for the relaxed elastomeric state is demonstrated by the β-spiral of Figure 3. Since the elastomeric state in the 40° to 60°C temperature range is a non-random (though dynamic) structured state, it follows that thermal denaturation should be observable. The dramatic (but very slow) expulsion of water from the coacervate on raising the temperature from 60° to 80°C seen in Figure 6 could be the result of denaturation of a water-containing structure. This can

be checked by circular dichroism studies in which the change in CD pattern on standing at 80°C is determined. This is shown in Figure 15. The recurring β-turn CD pattern is observed when the spectrum of the sample is determined shortly after reaching 80°C. On standing at 80°C, the CD pattern slowly reverts toward that of the low temperature (15°C) pattern (Urry, et al., 1985e). The 15°C CD pattern is obtained below the temperature for the onset of the inverse temperature transition and is indicative of a less ordered state. As the CD pattern on prolonged heating at 80°C slowly shifts toward that of a less ordered state, the process that occurs with expulsion of water in Figure 6 is shown to be denaturation. The half-life for denaturation in the small coacervate droplets of the CD study is about three days. Under these circumstances, the thermal denaturation can be easily shown to be reversible by lowering the temperature to 15°C where redissolution occurs.

It now becomes of particular interest to determine the effect of prolonged heating at 80°C on elastomeric force and on elastic modulus. Should denaturation result in significant losses of elastomeric force, then it would seem apparent that random chain networks would have little to do with the entropic elastomeric force of the PPP elastomer. In Figure 16, the stress/strain curve for the PPP elastomer is determined at 40°C to give an elastic modulus of 4.3×10^5 dynes/cm^2; the sample is then returned to zero extension, heated at 80°C for 24 hours while still in the stress/strain apparatus. The new length at zero force is determined at 40°C and the stress/strain curve is run at 40°C to 60% extension. The elastic modulus has decreased to 2.5×10^4 dynes/cm^2. In Figure 16, the 24 hour periods of heating at 80°C are repeated three more times and the elastic modulus determined after each 24 hour period. Heating at 80°C results in a loss of elastic modulus. In the inset in Figure 16 is a plot of the ln(elastic modulus) versus hours at 80°C from which a half-life of about 70

hours is obtained. This half-life is similar to that found in the circular dichroism study (see Figure 15). Interestingly there is also a shortening of the elastomer on heating at 80°C in analogy to the decrease in coacervate volume of Figure 6 above 60°C. Reversibility of the denaturation in the cross-linked condensed phase has not been demonstrated whereas for the CD study (Figure 15) and the composition study (Figure 6) reversibility was demonstrable by lowering the temperature to below 20°C where redissolution occurs after which the process can be repeated. Once the chains are denatured in the cross-linked sample, however, disentanglement has not been achieved even on swelling in water at 20°C or less. It may also be noted that when the thermoelasticity curves as in Figures 10 and 11 are run using four hours per data point above 40°C, then an irreversible loss of force is observed above 60°C. Thus thermal denaturation is demonstrable directly in terms of loss of elastomeric force. As thermal randomization of polypentapeptide chains results in loss of elastomeric force, clearly random chain networks are not responsible for the observed elastomeric force in the 40° to 60°C temperature range.

As an additional note, if the 40° to 60°C state is taken as the native state then heat denaturation is observed on raising the temperature above 60°C and cold denaturation is observed on lowering the temperature below 40°C. Interestingly however, cold denaturation results in a swelling of the elastomer whereas heat denaturation causes a shrinking of the elastomer.

F. Conclusions on the Mechanism of Entropic Polypentapeptide Elasticity

The preceding data clearly demonstrate that the classical theory of rubber elasticity, requiring as it does a random chain network, is not relevant to the entropic elasticity of the polypentapeptide of elastin. With respect to the possible contribution of solvent entropy to the entropic elastomeric force, there are a few points to note. It is expected that clathrate-like water would

form around the hydrophobic side chains exposed to solvent on stretching but the slow denaturation, the slow loss of elastomeric force at 80°C, is not of a time scale relevant to the formation and loss of clathrate-like water which occurs with a frequency in the GHz range (Buchet, et al., submitted) and the half-life for denaturation is the same whether the elastomer is heated at 80°C while stretched or while at zero extension (Urry, et al., submitted). Finally, as clathrate-like water has a weak temperature dependence (Buchet, et. al, submitted), there is little clathrate-like (low entropy) water at temperatures near 80°C and greater. It seems clear that force is borne by polypeptide chains and since denatured structure with randomized chains does not contribute significantly to the entropic elastomeric force exhibited in the 40° to 60°C temperature range, the only alternative source of chain entropy would be the entropy due to internal chain dynamics. This gives the librational entropy mechanism of elasticity.

IV. LIBRATIONAL ENTROPY MECHANISM OF ELASTICITY

A. Expressions of Entropy

Boltzmann's Relation: The state of a polypeptide or of a polypeptide segment can be completely specified by knowledge of the coordinates, q_i, and momenta, p_i, of each displaceable component. In this terminology, a peptide moiety or a methyl moiety may be considered a component. If n is the number of such components, then a state is specified by a single point in 2n dimensional (q_i, p_i) space, referred to as phase space. The number of a priori equally probable points (states), W, accessible to the system is a measure of the entropy of the system (Eyring, et al., 1961). This bridge between statistical mechanics and thermodynamics is called Boltzmann's relation and can be written

$$S = R \ln W \qquad (7)$$

where R is the gas constant, 1.987 cal/mole deg. Taking the peptide moiety to be planar and bond angles and lengths to be fixed, the state of a polypeptide backbone can also be considered to be completely specified with knowledge of the ϕ and ψ torsion angles . One state can be represented as a point in conformation space. The sum of accessible states can be represented by the volume occupied by such points. If the peptide segment of interest involved three torsion angles, then the range of torsion angle changes within a 1.5 kcal/mole cut-off energy (e.g. 0.5 kcal/mole for each degree of freedom) above the lowest energy state might be represented as ψ_1-ψ_1', ϕ_2-ϕ_2' and ψ_2-ψ_2'. Plotting these three amplitudes of torsion angle changes along each of three axes in a rectangular coordinate system describes a volume in three dimensional space and the volume would be proportional to the entropy of the peptide segment. Should there be n torsion angles, the space of interest would be n-dimensional and the volume of this conformation space would again be proportional to the entropy of the system. For the pentapeptide, (Val^1-Pro^2-Gly^3-Val^4-Gly^5), the ϕ(Pro) torsion angle would be fixed such that there would be nine backbone torsion angles. Considering the pentamer within the β-spiral conformation of Figure 3 and 4A to be the span from the Val^1 α-carbon of one repeat to the Val^1 α-carbon of the next repeat, the question of interest becomes how many ways can the pentamer segment span the gap from the position of one Val^1 α-carbon to the position of the next Val^1 α-carbon. Taking a 1 kcal/mole-residue cut-off energy and counting each 5° change in torsion angle as a new state, the number of states in the relaxed conformation (W^r), using the potential functions of Scheraga and coworkers (Momany, et al., 1974 and 1975), calculates to be 764 (Urry, et al., 1985f). Extending the β-spiral to 130% as shown in Figure 4B and using the same procedure as for the relaxed state, there calculated for the extended conformation to be 58 states, W^e. The change in entropy, ΔS, on deformation of the pentamer becomes

$$\Delta S = S^r - S^e = R \ln W^r/W^e \qquad (8)$$

$$= 1.987 \ln 764/58$$

$$= 5.12 \text{ cal/mole-deg per pentamer}$$

which is about one entropy unit per residue. To demonstrate that the entropy change is well-behaved with changes in cut-off energy, values of 0.6 and 2.0 kcal/mole have been used and the same values are obtained for the change in entropy. Alternatively, the Boltzmann summation overstates, $\sum_i e^{-\epsilon_i/RT}$, can be used in the statistical mechanical definition of entropy, i.e.,

$$S = R \ln \sum_i e^{-\epsilon_i/RT} + E/T$$

where ϵ_i is the energy per mole of each allowed state and E is the total internal energy. The change in entropy becomes

$$\Delta S = R \ln \left(\sum_i^r e^{-\epsilon_i^r/RT} \Big/ \sum_i^e e^{-\epsilon_i^e/RT} \right) + (E^r - E^e)/T \qquad (9)$$

Above it has been demonstrated that the polypentapeptide elastomer is almost entirely an entropic elastomer, i.e. that $f_e = 0$, which means that there is little change in internal energy on stretching such that $(E^r - E^e) = 0$. When the energy values for each state with a 5° change in torsion angle are used in the summations, the entropy change is again one entropy unit per residue (Urry, et al., 1985f). This demonstration of an entropy change due to the damping of internal chain dynamics is, of course, relevant to any sized peptide segment in which deformation can effect a damping of torsional motions.

Entropy of an Harmonic Oscillator: Another useful expression for entropy derives from the consideration of the frequency of motions. While these large amplitude, low frequency motions are expected to be highly anharmonic, useful qualitative insight is available from the statistical mechanical expression for entropy using the harmonic oscillator partition function (Dauber, et

al., 1981). The expression for entropy becomes

$$S_i = R\left[\ln(1 - e^{-h\nu_i/kT})^{-1} + \frac{h\nu_i}{kT}(e^{h\nu_i/kT} - 1)^{-1}\right] \qquad (11)$$

where ν_i is the frequency, k is the Boltzmann constant and h is Planck's constant (Eyring, et al., 1961). A plot of $\log\nu_i$ versus S_i (left hand ordinate) and TS_i (right hand ordinate) is given in Figure 17. What is apparent is that the lower the frequency, the larger the contribution to the entropy. A librational motion of 10 MHz frequency would contribute some 9 kcal/mole to the free energy. The correlation time, $\tau_i = \frac{1}{2\pi\nu_i}$, corresponding to 10 MHz is 16 nsec. This is more than two orders of magnitude longer than the currently longest trajectories calculable by means of molecular dynamics (Karplus and McCammon, 1981). With ultrasonic absorption of proteins showing a maximum in the 10 nsec range (Barnes, et al., 1985; Pethig, 1979; Zana and Tondre, 1972; Schneider, et al., 1969; Cho, et al., 1985; Cerf, 1985) and with the dielectric relaxation studies showing the importance of 10 nsec correlation times to entropic elasticity in polypeptides and proteins (Henze and Urry, 1985; Urry, et al., 1985), it is apparent that these low frequency motions have important contributions to the free energy and to the structure and function of proteins.

B. Lambda Plots and Peptide Librational Motions

As seen in Figure 4, it is the suspended, Val^4 α-carbon to Val^1 α-carbon, segment in which the larger amplitude torsional motions are apparent. Accordingly it becomes of interest to plot the allowed states on $\psi(Val^4)$ vs $\phi(Gly^5)$ and $\psi(Gly^5)$ vs $\phi(Val^1)$ maps. The four torsion angles of the suspended segment are paired as the torsion angles flanking each peptide moiety. The maps, called lambda plots, are given in Figure 18A for the relaxed conformation. Interestingly, each of the allowed states fall near a 45° diagonal, that is, whenever there is a change in ψ_i, there is a compensating, oppositely-signed change in ϕ_{i+1} (Urry, et al., 1982; Urry and Venkatachalam, 1983). The lambda

plots indicate that the peptide moieties are undergoing large amplitude rocking motions, i.e. peptide librations. This coupling of torsional angle changes is the basis for the identification of a librational entropy mechanism of elasticity. In the relaxed state, the amplitudes of the librations approach 180° whereas on a 130% extension along the spiral axis (about a 30% increase in the Val^{1}_{i} α-carbon - Val^{1}_{i+1} α-carbon distance) the amplitudes of the librations are severely damped to about one-third of the relaxed amplitude.

C. Dielectric Relaxation and the Amplitude of the Peptide Librational Process

As soon as the dynamic β-spiral in Figure 3 was derived (Venkatachalam and Urry, 1981), the concept of librational entropy was immediately raised due to the apparent freedom of the suspended segment (Urry, 1982), and tests of the concept were immediately initiated. These tests were the synthesis of the L·Ala^{5}-PPP and D·Ala^{5}-PPP analogs and the dielectric relaxation studies. The purpose of the former, replacing Gly^{5} by Ala^{5}, was to introduce a side chain, a CH_2 moiety, in the middle of the suspended segment to see if elasticity could be affected by the resulting limiting of peptide librations. The dielectric relaxation studies were to see if the librational process could be observed in PPP itself and, if observed, to see whether the librational amplitudes were damped in the Ala^{5}-PPP analogs. The L·Ala^{5}-PPP analog is inelastic in spite of essentially identical conformations and temperature profiles of aggregation; the product of the temperature induced aggregation is a granular precipitate rather than a viscoelastic coacervate, and the aggregation is irreversible (Urry, et al., 1983a). The D·Ala^{5}-PPP does form a viscoelastic coacervate (Urry, et al., 1983b). As noted above in Figure 12, the dielectric relaxation studies of PPP show a very interesting, low frequency, intense, and localized relaxation demonstrating a peptide librational process within a regular structure (Henze and Urry, 1985). Dielectric relaxation studies on the D·Ala^{5}-PPP coacervate

also demonstrate the relaxation but the amplitude is much reduced (Henze and Urry, unpublished data).

Using a series of cut-off energies, 0.6, 1.0, 1.5 and 2.0 kcal/mole-residue, the dipole moment change for a pentamer was computed for both PPP and D·Ala^5-PPP (Venkatachalam and Urry, 1986). For example at 1.5 kcal/mole-residue, the calculated dipole moment changes due to the librations were 3.78 Debye for PPP and 1.33 Debye for D·Ala^5-PPP. With these two values, it becomes of interest to use the Onsager equation for polar liquids (Onsager, 1931) to calculate the apparent dipole moment changes from the amplitudes of the dielectric relaxations. The dipole moment changes per pentamer approximated from the experimental data is 2 Debye for PPP and 0.7 Debye for D·Ala^5-PPP. Interestingly, the values of computed and approximated experimental dipole moment change due to the librations agree within a factor of two. Perhaps even more noteworthy is that the computed ratio of dipole moments 3.78/1.33 = 2.8, and the experimental ratio of the dielectric increments per mole pentamer at the 40°C coacervate concentrations, (72/2) (33/2.5) = 2.7, are essentially identical. Thus the comparison of computed librational processes to experimental results is favorable. This provides the desired comparison of a calculated and experimental result on a property that is experimentally shown (see Figure 10) to be directly proportional to the magnitude of entropic elastomeric force.

V. SUMMARIZING COMMENTS

Prior to the studies briefly reviewed here on the polypentapeptide of elastin (see Part III), entropic protein elasticity was considered to require networks of random chains (Hoeve and Flory, 1974), that is, to be described by the classical theory of rubber elasticity. To have entropic elastomeric force exhibited by the more-ordered state (the higher temperature state) resulting from an inverse temperature transition, as demonstrated by the polypentapeptide

of elastin studies, is, of course, contradictory to the random chain network requirement. Thus to be able to vary the temperature for the development of elastomeric force by varying the hydrophobicity of a polypeptide sequence is a new concept. Clearly as required for an inverse temperature, that an increase in the hydrophobicity of the polypeptide sequence causes the transition to shift to a lower temperature and that a decrease in the hydrophobicity causes the transition to shift to a higher temperature has been demonstrated. This means at a fixed temperature that it should be possible to turn "on" and "off" elastomeric force exhibited by a protein by reversibly changing the polarity of such a polypeptide sequence. The polarity of polypeptide chains can be changed by means of a chemical process. Thus, the mechanism, called mechanochemical coupling of the first kind, becomes a new consideration for understanding protein mechanisms where elastic forces are involved.

Having demonstrated that protein elasticity does not require random chain networks and, in fact, having shown that thermal denaturation of an elastic protein results in dramatic loss of elastic modulus suggest that descriptions of protein elastic processes should not invoke random coils. Thermal denaturation of elastin and the polypentapeptide of elastin results in essentially complete loss of useful restoring forces. Thermally denatured polypentapeptide of elastin (random coil elastin) neither effectively resists nor recovers from deformation when denaturation is carried out while extended. Accordingly in those cases where the transition to the elastic state is a regular transition from a stiff lower entropy state to a higher entropy state with a useful elastic modulus, it now seems necessary to consider conformational states intermediate in entropy between α-helices for example and random coils. Consideration of the conformation of that intermediate entropy state, particularly when achieved using repeating peptide sequences, should include spiral conformations in which the repeating sequence as a conformational entity repeats on a helical axis.

Whatever the conformation, it is argued that the entropy of the intermediate state should be described in terms of internal chain dynamics, i.e., librational motions, instead of networks of random chains with a random distribution of end-to-end chain lengths. As it would be a situation requiring that the same repeating sequence be compatible with two different non-random conformations, it would be a situation more demanding of the protein sequence. This more involved process for turning "on" and "off" elastomeric force will then be called mechanochemical coupling of the second kind. Again a chemical process is sought that will shift the temperature of the transition as the mechanism to turn "on" and "off" the elastomeric force.

Important to the understanding of elastic processes in globular proteins is the demonstration that entropic elastomeric force is the result of internal chain dynamics and that a short peptide segment of but a few residues can exert an entropic elastomeric force. Because of this, the above considerations of obvious relevance to fibrillar proteins now become relevant to globular proteins. A short peptide segment can exhibit a large entropy due to internal chain dynamics with the ends of the segment fixed in space, and with the ends fixed in space, the internal motions become describable in terms of librations in which the change in one torsion angle is compensated by an oppositely signed change in one or more other torsion angles. This is called the librational entropy mechanism of elasticity. Any change in the segment that results in a decrease in amplitude and/or an increase in the frequency of the motion will result in an entropic elastomeric force being exerted at the points of attachment of segment to additional structure. The change could be a mechanical process such as stretching (an increase in end-to-end length of the segment), it could be a chemical process as in the mechanochemical coupling considered above, or it could be an electrical process as the effect of an electric field on a membrane protein.

ACKNOWLEDGEMENT

The author wishes to acknowledge the many members of the Laboratory of Molecular Biophysics, past and present, that have contributed so extensively to the work reviewed here. This work was supported in part by National Institutes of Health grant HL 29578 and Department of the Navy, Office of Naval Research contract N00014-86-K-0402.

References:

Aaron, B. B. and Gosline, J. M. (1981). Biopolymers 20, 1247-1260.

Aaron, B. B. and Gosline, J. M. (1980). Nature 287, 865-867.

Andrady, A. L. and Mark, J. E. (1980). Biopolymers 19, 849-855.

Barnes, C., Evans, J. A. and Lewis, T. J. (1985). J. Acoust. Soc. Am. 78(1), 6-11.

Buchet, R., Luan, C.-H., Prasad, K. U., Harris, R. D. and Urry, D. W. (Submitted).

Bungenberg de Jong, H. G. (1949). In Colloid Science, Vol. 2 (Kruyt, H. R., ed.) Elsevier/North Holland Publishers, Amsterdam, pp. 232-258.

Bungenberg de Jong, H. G. and Kruyt, H. R. (1930). Kolloid-Z 50, 39-48.

Bungenberg de Jong, H. G. and Kruyt, H. R. (1929). Proc. Kon. Ned. Adak. Wet. 32, 849-856.

Cerf, R. (1985). Biophys. J. 47, 751-756.

Cho, K. C., Leung, W. P., Mok, H. Y. and Cjoy, C. L. (1985). Biochim. Biophys. Acta 830, 36-44.

Cleary, E. G. and Moont, M. (1977). Adv. Exp. Med. Biol. 79, 477-490.

Cook, W. J., Einspahr, H. M., Trapane, T. L., Urry, D. W. and Bugg, C. W. (1980). J. Am. Chem. Soc. 102, 5502-5505.

Dauber, P., Goodman, M., Hagler, A. T., Osguthorpe, D., Sharon, R. and Stern, P. (1981). In ACS Symposium Series, No. 173 Supercomputers in Chemistry (Lykos, P. and Shavitt, I., eds.) pp. 161-191.

Dorrington, K. L. and McCrum, N. G. (1977). Biopolymers 16, 1201-1222.

Eyring, H., Henderson, D., Stover, B. J. and Eyring, E. M. (1961). Statistical Mechanics and Dynamics, p. 90.

Eyring, H. (1932). Phys. Rev. 39, 746-748.

Fleming, W. W., Sullivan, C. E. and Torchia, D. A. (1980). Biopolymers 19, 597-618.

Flory, P. J., Ciferri, A. and Hoeve, C. A. J. (1960). J. Polymer Sci. 45, 235-236.

Flory, P. J. (1953). Principles of Polymer Chemistry, Cornell University Press, Ithaca.

Frank, H. S. and Evans, M. W. (1945). J. Chem. Phys. 13, 493-407.

Franzblau, C. and Lent, R. W. (1969). In Brookhaven Symposium in Biology: Structure, Function and Evolution in Proteins, Vol. 2, pp. 358-377.

Gosline, J. M. and Rosenbloom, J. (1984). In Extracellular Matrix Biochemistry (Piez, K. A. and Reddi A. H., eds.) Elsevier/North Holland Publishers, Amsterdam, pp. 191-227.

Gosline, J. M. (1980). In The Mechanical Properties of Biological Materials (Vincent, J. F. V. and Currey, J. D., eds.) Cambridge University Press, London, pp. 331-357.

Gosline, J. M. (1978). Biopolymers 17, 677-695.

Gray, W. R., Sandberg, L. B. and Foster, J. A. (1973). Nature 246, 461-466.

Henze, R. and Urry, D. W. (1985). J. Am. Chem. Soc. 107, 2991-2993.

Hoeve, C. A. J. and Flory, P. J. (1958). J. Am. Chem. Soc. 80, 6523-6526.

Hoeve, C. A. J. and Flory, P. J. (1974). Biopolymers 13, 677-686.

Karplus, M. and McCammon, J. A. (1981). CRC Critical Reviews in Biochem. 9, 293-349.

Kauzmann, W. (1959). Adv. Protein Chem. 14, 1-63.

Lyerla, J. R. and Torchia, D. A. (1975). Biochemistry 13, 5175-5183.

Mandelkern, L. (1983). An Introduction to Macromolecules, 2nd ed., Springer-Verlag, Inc., New York.

Momany, F. A., McGuire, R. F., Burgess, A. W. and Scheraga, H. A. (1975). J. Phys. Chem. 7, 2361-2381.

Momany, F. A., Carruthers, L. M., McGuire, R. F. and Scheraga, H. A. (1974). J. Phys. Chem. 78, 1595-1620.

Onsager, L. (1931). Phys. Rev. 37, 405-426.

Partridge, S. M. (1962). Adv. Prot. Chem. 17, 227-302.

Pethig, R. (1979). In Dielectric and Electronic Properites of Biological Materials, John Wiley and Sons, Inc., New York, pp. 100-149.

Petruska, J. A. and Sandberg, L. B. (1968). Biochem. Biophys. Res. Commun. 33, 222-228.

Queslel, J. P. and Mark, J. E. (1986). In Encyclopedia of Polymer Science and Engineering Vol. 5, Second edition, John Wiley and Sons, Inc., pp. 365-408.

Rosenbloom, J. Private communication.

Sandberg, L. B., Soskel, N. T. and Leslie, J. B. (1981). N. Engl. J. Med. 304, 566-579.

Sandberg, L. B., Gray, W. R. and Franzblau, C. (1977). Adv. Exp. Med. Biol. 79, 259-261.

Schneider, F., Müller-Landau, F. and Mayer, A. (1969). Biopolymers 8, 537-544.

Swaminathan, S., Harrison, S. W. and Beveridge, D. L. (1978). J. Amer. Chem. Soc. 100, 5705.

Tanford, C. (1973). The Hydrophobic Effect: Formation of Micelles and Biological Membranes, John Wiley and Sons, Inc., New York.

Thomas, G. J., Jr., Prescott, B. and Urry, D. W. Biopolymers (in press).

Torchia, D. A., Batchelder, L. S., Fleming, W. W., Jelinski, L. W., Sarkar, S. K. and Sullivan, C. E. (1983). In Mobility and Function in Proteins and Nucleic Acids (Porter, R., O'Connor, M. and Whelan, J., eds.) Pitman Publishers, London, pp. 98-115.

Torchia, D. A. and Piez, K. A. (1973). J. Mol. Biol. 76, 419-424.

Urry, D. W. (1972). Proc. Natl. Acad. Sci. USA 69, 1610-1614.

Urry, D. W. (1974). In Arterial Mesenchyme and Arteriosclerosis (Wagner, W. D. and Clarkson, T. B., eds.) Plenum Publishing Corporation, New York, Adv. Exp. Med. Biol. 43, pp. 211-243.

Urry, D. W. (1982). In Methods in Enzymology (Cunningham, L. W. and Frederiksen, D. W., eds.) Academic Press, Inc., New York, New York 82, pp. 673-716.

Urry, D. W. (1983). Ultrastruct. Pathol. 4, 227-251.

Urry, D. W. (1984). J. Protein Chem. 3, 403-436.

Urry, D. W. (1985). In Biomolecular Stereodynamics III (Sarma, R. H. and Sarma, M. H., eds.) Adenine Press, Guilderland, New York, pp. 173-196.

Urry, D. W. Presented at Partridge Symposium (Laurea Honoris Causa), University of Padova, 1986, Scottish Academic Press (in press).

Urry, D. W. and Long, M. M. (1976). CRC Crit. Rev. Biochem. 4, 1-45.

Urry, D. W. and Prasad, K. U. (1985). In Biocompatibility of Tissue Analogues (Williams, D. F., ed.) CRC Press, Inc., Boca Raton, Florida, pp. 89-116.

Urry, D. W. and Venkatachalam, C. M. (1983). Int. J. Quantum Chem.: Quantum Biol. Symp. No. 10, 81-93.

Urry, D. W., Okamoto, K., Harris, R. D., Hendrix, C. F. and Long, M. M. (1976). Biochemistry 15, 4083-4089.

Urry, D. W., Khaled, M. A., Rapaka, R. S. and Okamoto, K. (1977) Biochem. Biophys. Res. Commun. 79, 700-706.

Urry, D. W., Venkatachalam, C. V., Long, M. M. and Prasad, K. U. (1982). In Conformation in Biology (Srinivasan, R. and Sarma, R. H., eds.) G. N. Ramachandran Festschrift Volume, Adenine Press, USA, pp. 11-27.

Urry, D. W., Trapane, T. L., Long, M. M. and Prasad, K. U. (1983a). J. Chem. Soc., Faraday Trans. I 79, 853-868.

Urry, D. W., Trapane, T. L., Wood, S. A., Walker, J. T., Harris, R. D. and Prasad, K. U. (1983b). Int. J. Pept. Protein Res. 22, 164-175.

Urry, D. W., Henze, R., Harris, R. D. and Prasad, K. U. (1984). Biochem. Biophys. Res. Commun. 125, 1082-1088.

Urry, D. W., Henze, R., Redington, P., Long, M. M., Prasad, K. U. (1985a). Biochem. Biophys. Res. Commun. 128, 1000-1006.

Urry, D. W., Prasad, K. U., Trapane, T. L., Iqbal, M., Harris, R. D. and Henze, R. (1985b). Polymeric Materials: Sci. and Engineering 53, 241-245.

Urry, D. W., Shaw, R. G. and Prasad, K. U. (1985c). Biochem. Biophys. Res. Commun. 130, 50-57.

Urry, D. W., Trapane, T. L., Iqbal, M., Venkatachalam, C. M. and Prasad, K. U. (1985d). Biochemistry 24, 5182-5189.

Urry, D. W., Trapane, T. L. and Prasad, K. U. (1985e). Biopolymers 24, 2345-2356.

Urry, D. W., Venkatachalam, C. M., Wood, S. A. and Prasad, K. U. (1985f). In Structure and Motion: Membranes, Nucleic Acids and Proteins (Clementi, E., Corongiu, G., Sarma, M. H. and Sarma, R. H., eds.) Adenine Press, Guilderland, New York, pp. 185-203.

Urry, D. W., Harris, R. D., Long, M. M. and Prasad, K. U. (1986a). Int. J. Pept. and Protein Res. 28, 649-660.

Urry, D. W., Haynes, B. and Harris, R. D. (1986b). Biochem. and Biophys. Res. Commun. 141, 749-755.

Urry, D. W., Long, M. M., Harris, R. D. and Prasad, K. U. (1986c). Biopolymers 25, 1939-1953.

Urry, D. W., Trapane, T. L., McMichens, R. B., Iqbal, M., Harris, R. D. and Prasad, K. U. (1986d). Biopolymers 25, S209-S228.

Urry, D. W., Prasad, K. U., Trapane, T. L., Iqbal, M., Harris, R. D., Okamoto, K. and Henze, R., Peptide Chem. (in press).

Urry, D. W., Chang, D. K., Krishna, R., Huang, D. H., Trapane, T. L. and Prasad, K. U. (in preparation, a).

Urry, D. W., Haynes, B. and Harris, R. D. (in preparation, b).

Venkatachalam, C. M. and Urry, D. W. (1981). Macromolecules 14, 1225-1229.

Venkatachalam, C. M. and Urry, D. W. (1986). Int. J. Quantum Chem.: Quantum Biol. Symp. 12, 15-24.

Volpin, D., Urry, D. W., Pasquali-Ronchetti, I. and Gotte, L. (1976). Micron 7, 193-198.

Weis-Fogh, T. and Andersen, S. A. (1970). Nature 227, 718-721.

Zana, R. and Tondre, C. (1972). J. Phys. Chem. 76, 1737-1743.

Figure Legends:

Figure 1 A fifty segment random chain in two dimensions with allowed angles ranging from +90° to -90° and with the end-to-end distance vector indicated as r. Reproduced with permission from Flory, 1953.

Figure 2 Distribution, W(r), of end-to-end chain lengths for a freely jointed chain of 10,000 segments each of 0.25 nm in length. The most probable end-to-end length is near 20 nm with occurrences ranging from overlapping of ends to the fully extended chain. Redrawn from Flory, 1953 and Queslel and Mark, 1986. The dashed line is a schematic representation of the distribution of end-to-end chain lengths that could occur for well-oriented 800 residue polypentapeptide of elastin in the β-spiral conformation when in an unstretched cross-linked elastomeric matrix. It is the *unwinding* of a β-spiral structure in the cross-linked matrix on reversing the inverse temperature transition, i.e., on lowering the temperature from 40° to 20°C, that results in an increase in length of the elastomer by more than 200% (see Figure 13).

Figure 3 Molecular Structure of the Polypentapeptide of Elastin

A. β-turn of the pentamer, Val^1-Pro^2-Gly^3-Val^4-Gly^5, with the Val^1C-O...HNVal^4 10 atom hydrogen bonded ring, with the Pro^2-Gly^3 sequence at the corners of the turn and with the intervening peptide moiety with its C-O, the Pro C-O, directed on the side opposite to that of the Pro α-CH. This is called a type II Pro^2-Gly^3 β-turn. Adapted with permission from Cook, et al., 1980.

B. Schematic representation of a helical structure with the helical parameters those of the β-spiral of the PPP.

C. Schematic representation of the β-spiral showing the β-turns functioning as spacers between the turns of the helix (spiral). The β-spiral is the result of optimizing intramolecular hydrophobic interactions.

D. Spiral axis view in stereo pair of a detailed plot showing one of a class of closely related β-spiral conformations. There is room for several columns of water within the β-spiral and shown suspended between β-turns is the suspended peptide segment within which the peptide moieties can undergo large amplitude rocking motions. B, C and D reproduced with permission from Urry, 1983.

E. Stereo pair side view showing one of a class of closely related β-spiral conformations (the same as in D). β-turns are seen to function as spacers between turns of the spiral with the interturn contacts utilizing the hydrophobic Val and Pro side chains. There are spaces in the surface of the β-spiral where intraspiral water can exchange with extraspiral water. The suspended segments are seen to be essentially surrounded by space to be filled with water, and are therefore free to exhibit large librational motions (see Figure 4). Reproduced with permission from Venkatachalam and Urry, 1981.

F. Stereo pair of supercoiling of three β-spirals in αC-αC virtual bond representation.

G. Stereo pair representing the structure resulting from supercoiling of three β-spirals. The residues are represented as spheres of different radii centered on the α-C of different residues.

This approximates the twisted filaments seen in Figure 8A., F. and G. reproduced with permission from Urry, et al., 1982.

Figure 4 Stereo pair representation of a pentadecapeptide fragment in (A) relaxed and (B) extended (130%) states. A central pentamer from the Val^1 α-carbon of one repeat to the Val^1 α-carbon of the next repeat is shown with the maximal torsional oscillations allowed for a 2 kcal/mole-residue cut-off energy. Note the large amplitude rocking possible in A and the greatly damped rocking on stretching in B. This shows the decrease in backbone entropy that occurs on extension. Reproduced with permission from Urry and Venkatachalam, 1983.

Figure 5 Temperature profiles for aggregation followed as the development of turbidity at 300 nm on raising the temperature of a range of concentrations of polypentapeptide. As the concentration is raised, aggregation begins at an increasingly lower temperature and exhibits a steeper rise in turbidity until a high concentration limit is reached above which increases in concentration cause no further lowering of temperature. The temperature of the high concentration limit can be used in a plot vs ln molecular weight to estimate molecular weight. Reproduced with permission from Urry, et al., 1985e.

Figure 6 Composition study of the polypentapeptide-water system as a function of temperature. At 20°C, the polypentapeptide and water are miscible in all proportions. At 30°C, a phase separation has occurred in which the more dense phase, called the coacervate, is 37% peptide, 63% water by weight. The overlying equilibrium solution, which contains more peptide the lower the molecular weight of the polypentapeptide, can be removed and the tube resealed. From

40° to 60°C there is the expression from the coacervate of very little equilibrium solution. Above 60°C however there is a dramatic release of water from the coacervate phase indicating a second transition. It will be shown by circular dichroism that this corresponds to a decrease in intramolecular order. Reproduced with permission from Urry, (in press).

Figure 7 Phase-structure diagram of the polypentapeptide water system developed primarily from the data of Figure 6 and supplemented by other physical characterizations. Adapted with permission from Urry, 1985.

Figure 8 Self-Assembly into Filaments, Fibrils and Fibers

A. Aggregates from the cloudy solution of Figure 5 prepared for examination in transmission electron microscope using the *negative staining* technique. The molecules dissolved in water below 25°C aggregate on raising the temperature to form filaments. Optical diffraction of the micrograph shows a major equatorial reflection near 5 nm which corresponds to the interfilament distance. At about 40° off the meridian is another spot suggesting a twist to the filament as may be observed directly on close examination of the micrograph. The twisted filaments are modelled using polypentapeptide β-spirals in Figure 3E and F. Reproduced with permission from Volpin, et al., 1976.

B. Polypentapeptide chemically cross-linked during the aggregation of the inverse temperature transition is seen in the scanning electron microscope to have self-assembled into fibers comprised of parallel aligned fibrils (see text for more detail). Reproduced with permission from Urry, et al., 1976.

Figure 9 Preparation and characterization of the cross-linked polypentapeptide. When polypentapeptide coacervate is formed in a tube as in Figure 6 and the 40°C composition is γ-irradiation cross-linked using a 20 x 10^6 radiation absorbed dose (20 MRAD), an elastomeric cylinder is prepared as shown in A. The elastomeric cylinder can be racked up as in B for NMR studies. A plot of the temperature dependence of peptide $^{15}\underline{NH}$ correlation time of ^{15}N Gly^5-PPP is shown in C for both coacervate (solid line) and elastomeric cylinder (dashed line). The inverse temperature transition is seen as a decrease in backbone mobility on going from 20° to 40°C. At temperatures above the transition, the temperature dependence of correlation time plotted vs T^{-1} (°K) shows an energy barrier to backbone motion of about 1.5 kcal/mole for both the coacervate and the elastomer. Reproduced with permission from Urry, et al., 1986d. D. Synthetic elastomeric band prepared on 20 MRAD cross-linking of coacervate band formed within the channel of a pestle when in a cryotube as in E.

Figure 10 Thermoelasticity data (solid line, left-hand ordinate) and dielectric permittivity, real part at 3.9 MHz (dashed line, right-hand ordinate) on the polypentapeptide of elastin. Both sets of data have been divided by the absolute temperature (°K). For the thermoelasticity study, the 40°C coacervate concentration was 20 MRAD cross-linked; the resulting elastomeric band was stretched to 63% at 40°C and the elastomeric force measured as a function of temperature. The dramatic rise in force between 25° and 40°C is due to the inverse temperature transition (i.e., elastomeric force increases on increasing order) and the near zero slope above 40°C indicates a dominantly entropic elastomer.

For the dielectric relaxation study, a 40°C coacervate was injected from below into a coaxial line cell and the dielectric permittivity (real part) was determined as a function of temperature over the 1 MHz to 1 GHz frequency range (see Figure 12A). In this Figure, the real part of the dielectric permittivity at 3.9 MHz divided by the absolute temperature (°K) is plotted as a function of temperature. The development of the local intense relaxation centered above 10 MHz (see Figure 12) correlates with the development of elastomeric force. Thus the development of a regular structure in which the peptide moieties are librating near a 10 MHz frequency is responsible for the force development.

Figure 11 Ellipticity data at 197 nm of the polypentapeptide of elastin in water (2.3 mg/ml) as a function of temperature (left-hand ordinate). The ellipticity changes from that more indicative of a less ordered state at 20°C to that indicative of a recurring β-turn conformation at 40°C and above. On the right hand ordinate is plotted the force as a function of temperature for a cross-linked band of polypentapeptide having been stretched to 60% at 40°C. Elastomeric force development correlates with development of intramolecular order as monitored by circular dichroism. Reproduced with permission from Urry, et al., 1985c.

Figure 12 Dielectric relaxation study of the 40°C concentration of polypentapeptide coacervate in the 1 MHz to 1 GHz frequency range.

A. As the temperature is raised above 20°C, an intense, local relaxation develops above 10 MHz (Henze and Urry, unpublished data).

B. The 40°C minus 20°C difference curve compared to a Debye-type curve (difference curve from the data of Henze and Urry,

1985). The close superposition indicates a remarkably localized frequency requiring a regular structure. The relaxation has been assigned to a peptide librational mode. As shown in Figure 10 using the 3.9 MHz data point from part A, the intensity of this relaxation correlates with the development of elastomeric force.

Figure 13 Temperature dependence of length under zero load of the 20 MRAD cross-linked 40°C coacervate concentration of the polypentapeptide of elastin (curve a). Note the dramatic shortening (contraction) that occurs on raising the temperature from 20° to 40°C. The magnitude of this shortening is equivalent to taking a near extended polypentapeptide chain with β-turns in place and wrapping it up into the β-spiral shown in Figure 3. This shortening is due to an inverse temperature transition in which intramolecular hydrophobic interactions are optimized. Note that a classical rubber, latex, uniformly expands as the temperature is raised without load (curve c). In curve b is the data for ligamentum nuchae elastin which also shows the inverse behavior, over a broader range but again most steeply in the 20° to 40°C temperature range. Curves a and c are not those exhibited by random chain networks. Reproduced with permission from Urry, et al., 1986b.

Figure 14 Effect of polypeptide hydrophobicity on the temperature range of the inverse temperature transition and the temperature range for the development of elastomeric force for Ile^1-PPP $(Ile^1\text{-}Pro^2\text{-}Gly^3\text{-}Val^4\text{-}Gly^5)_n$, for PPP $(Val^1\text{-}Pro^2\text{-}Gly^3\text{-}Val^4\text{-}Gly^5)_n$ and for PTP $(Val^1\text{-}Pro^2\text{-}Gly^3\text{-}Gly^4)_n$, where all polypeptides are greater than 50,000 molecular weight.

A. Temperature profiles for aggregation as a function of concentration for each of the three sequential polypeptides.

B. Ellipticity data showing the increase in order as a function of temperature for each of the three sequential polypeptides.

C. Development of elastomeric force as a function of temperature for each of the three sequential polypeptides after γ-irradiation in their coacervate states.

The addition of a single CH_2 moiety within the pentamer increases the pentamer hydrophobicity and shifts the intermolecular hydrophobic interaction (A), shifts the intramolecular hydrophobic interaction (B) and shifts the development of elastomeric force to lower temperature. (Adapted with permission from Urry, et al., 1986_.) The deletion of the hydrophobic Val^4 residue shifts the aggregation, the increase in intramolecular order and the development of elastomeric force to higher temperature. (Adapted with permission from Urry, et al., 1986a,c.) The magnitudes in the shifts are proportional to the hydrophobicity change (Urry, et al., 1986a). Thus the temperature range over which elastomeric force develops can be shifted by changing the hydrophobicity of the polypeptide.

Figure 15 Circular Dichroism data on the polypentapeptide of elastin for 2.3 mg/ml in water. At 15°C, the CD pattern is characteristic of polypeptides with less order. A random polypeptide would have value of -4×10^4 at 195 nm and a slightly positive or no band near 220 nm. The presence of a negative band near 220 nm and the -1.1×10^{-4} band near 200 nm suggests the presence of some order even at 15°C. On steadily raising the temperature to 80°C, the pattern changes to one characteristic of a repeating Type II β-

turn. However on standing at 80°C, the pattern slowly changes back toward that of less order. This slow denaturation is entirely reversible by lowering the temperature below 25°C.

Figure 16 Stress/strain data on the 20 MRAD cross-linked 40°C coacervate concentration of the polypentapeptide as a function of time at 80°C and zero extension. The first stress/strain cycle to 60% elongation and back, determined at 40°C gave an elastic modulus of 4.3×10^5 dynes/cm^2. The sample at zero extension was then held at 80°C for 24 hours after which the elastic modulus was again determined at 40°C to be 2.5×10^5 dynes/cm^2. This procedure was repeated three more times. After each 24 hours of heating at 80°C, the elastic modulus decreased. In the insert is a plot of ln(elastic modulus) versus time in hours at 80°C. From the plot, the half-life for thermal denaturation could be determined to be about 70 hours similar to that seen in Figure 15. Interestingly in relation to the data in Figure 6, the elastomeric band also shortens on standing at 80°C. While the effect of prolonged heating at 80°C seen in Figures 6 and 15 are reversible, in the condensed cross-linked matrix where low temperature dissolution are not possible, reversibility has not been demonstrated. Polypeptide chains once randomized in condensed phases apparently do not readily restructure. Importantly the effects of thermal denaturation are directly observable as a loss of elastomeric force.

Figure 17 Plot of Equation 11 for the entropy S_j in cal/mole-deg on the left-hand ordinate and given as TS_j in kcal/mole on the right-hand ordinate. This demonstrates the increasing contribution of low frequency motions to the entropy of a polypeptide chain.

Figure 18 Lambda plots of peptide moieties in the suspended segment of the β-spiral of the polypentapeptide of elastin in the relaxed A and extended B states and for the D·Ala^5 analog in the relaxed state C. When the $\psi(Val_4)$ torsion angle is plotted versus the $\phi(Gly_5)$ torsion angle and similarly for the $\psi(Gly_5)$ versus the $\phi(Val_1)$, all of the allowed conformational states within a 2 kcal/mole-residue cut-off energy fall on a 45° diagonal. This means that these pairs of torsion angles are correlated and that the peptide moieties undergo rocking motions, called librations. In the relaxed state, these librational motions can occur with large changes in torsion angle approaching 180°. When stretched to 130%, however, the amplitudes of the motion are greatly damped as seen in B where the magnitude of the changes in torsion angles within the same cut-off energy is now reduced to about one-third. For the D·Ala^5-PPP in its relaxed state, the plots of $\psi(Val_4)$ vs $\phi(D\cdot Ala_5)$ and $\psi(D\cdot Ala^5)$ vs $\phi(Val_1)$ in C, the range of allowed torsion angles is also markedly decreased over those for the PPP in A. This decreased motion for the same 2 kcal/mole-residue cut-off energy obtained on the basis of the conformational energy calculations is observed in the dielectric relaxation studies (see text for discussion). A and B reproduced with permission from Urry, et al., 1982 and Urry and Venkatachalam, 1983; and C reproduced with permission from Venkatachalam and Urry, 1986.

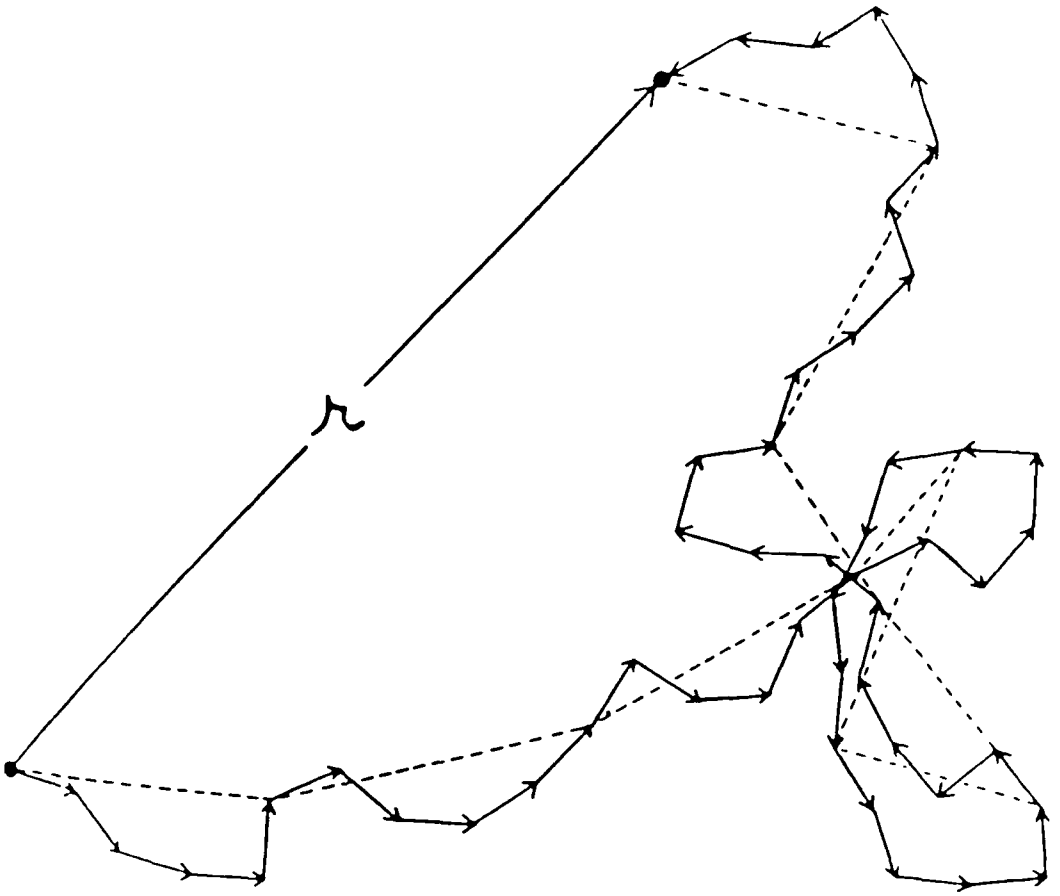

FIGURE 1

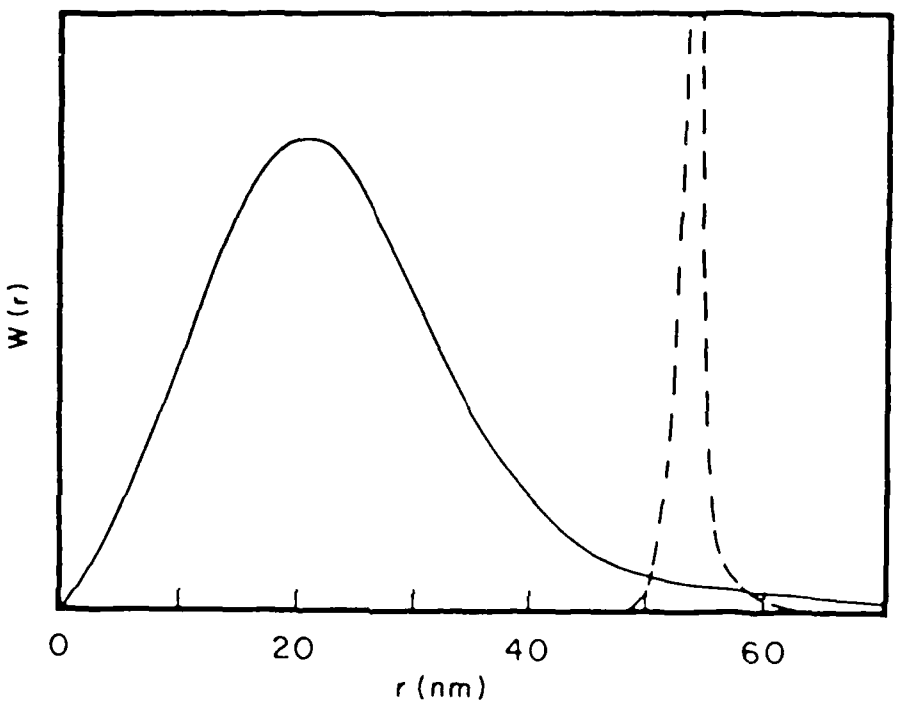

FIGURE 2

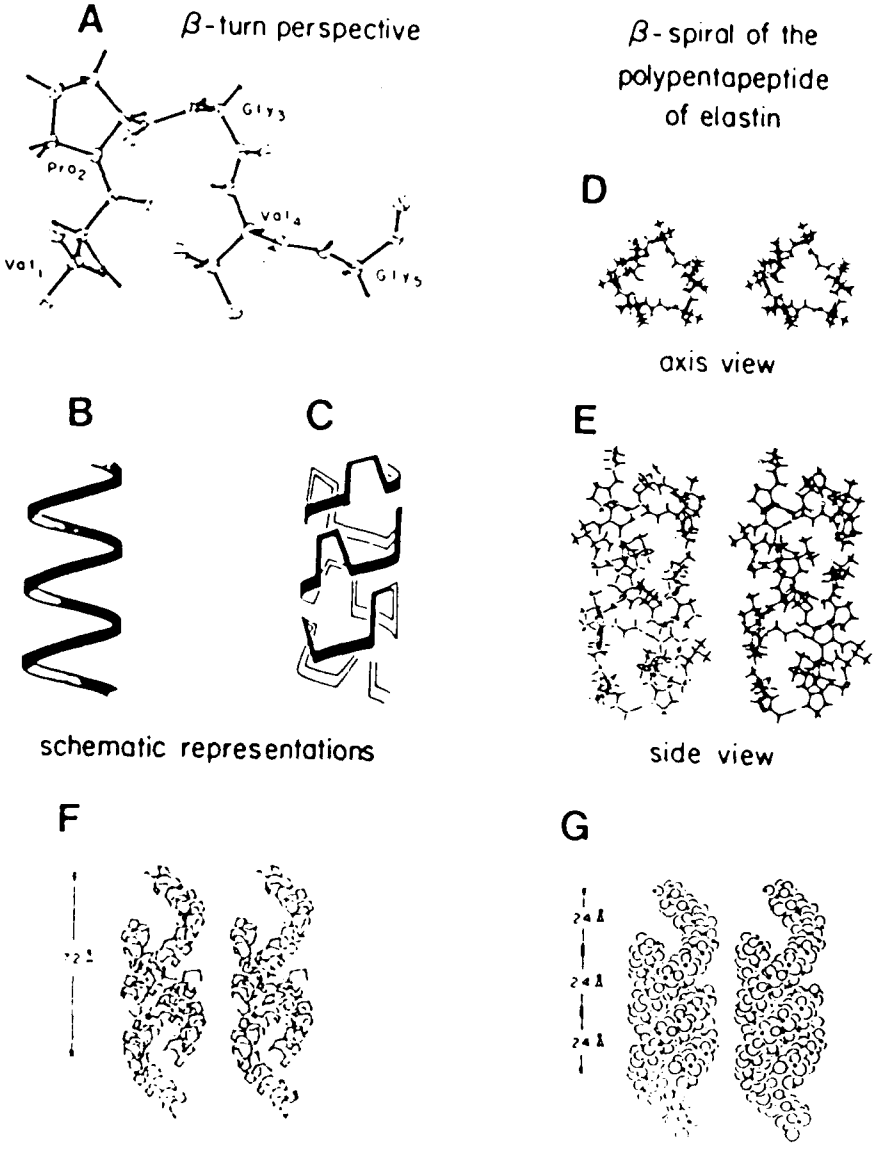

twisted filament (super coiled) representations

FIGURE 3

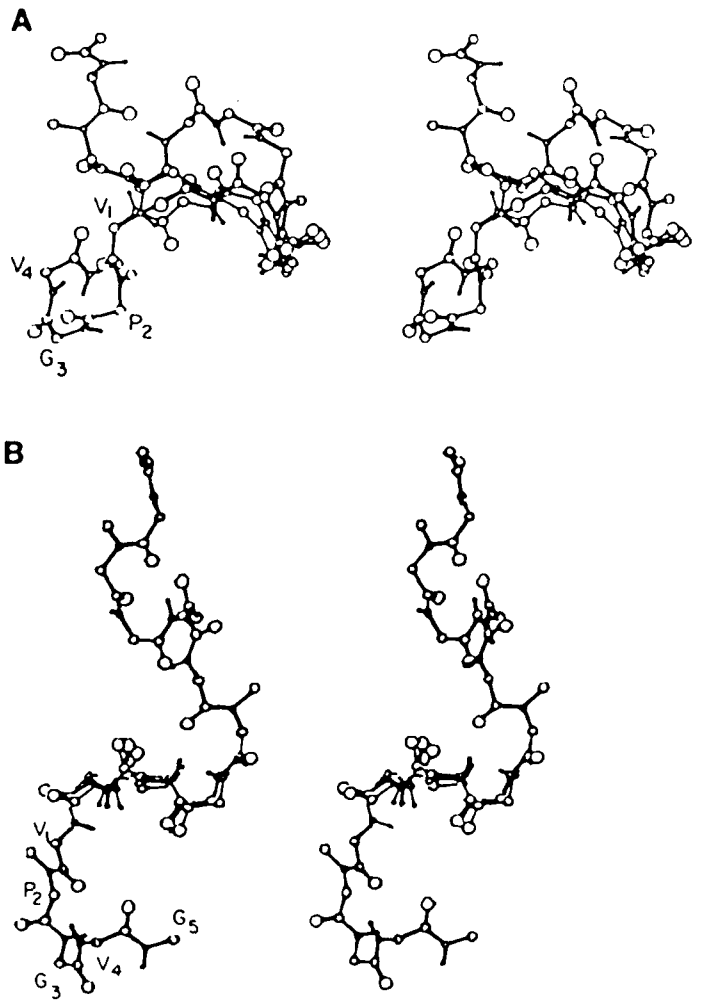

FIGURE 4

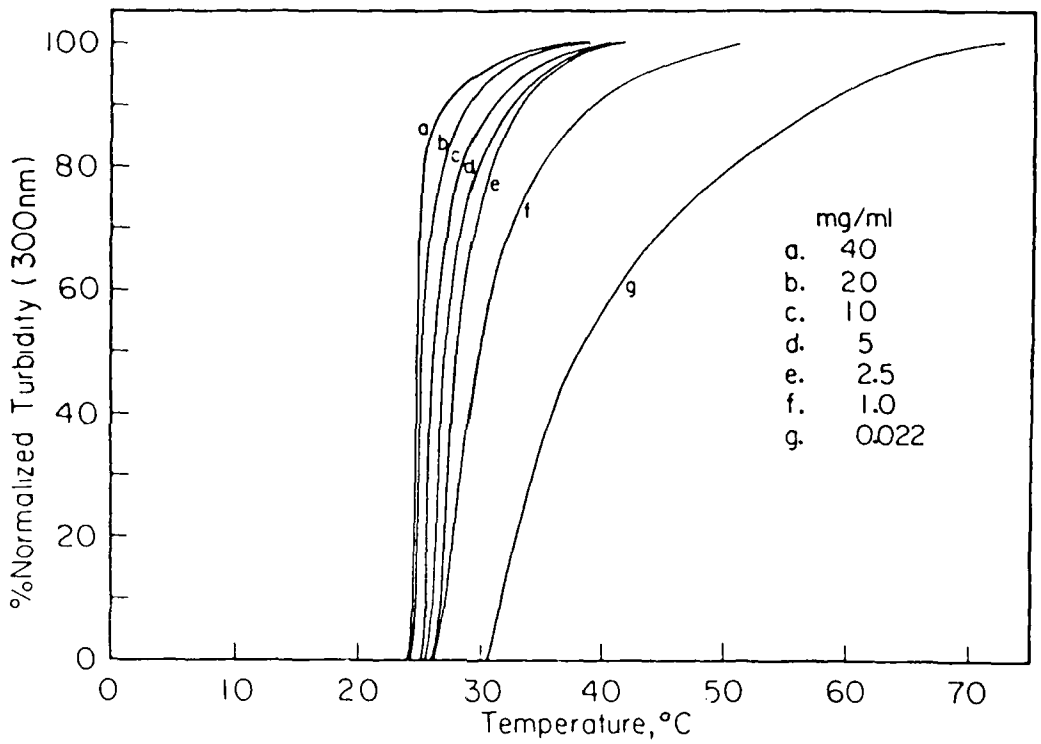
%Normalized Turbidity (300nm)
100
80
60
40
20
0
0
10
20
30
40
50
60
70
Temperature, °C
a
b
c
d
e
f
g
mg/ml
a. 40
b. 20
c. 10
d. 5
e. 2.5
f. 1.0
g. 0.022

FIGURE 5

Polypentapeptide + Water

Coacervation and Temperature

Dependence of Coacervate Concentration

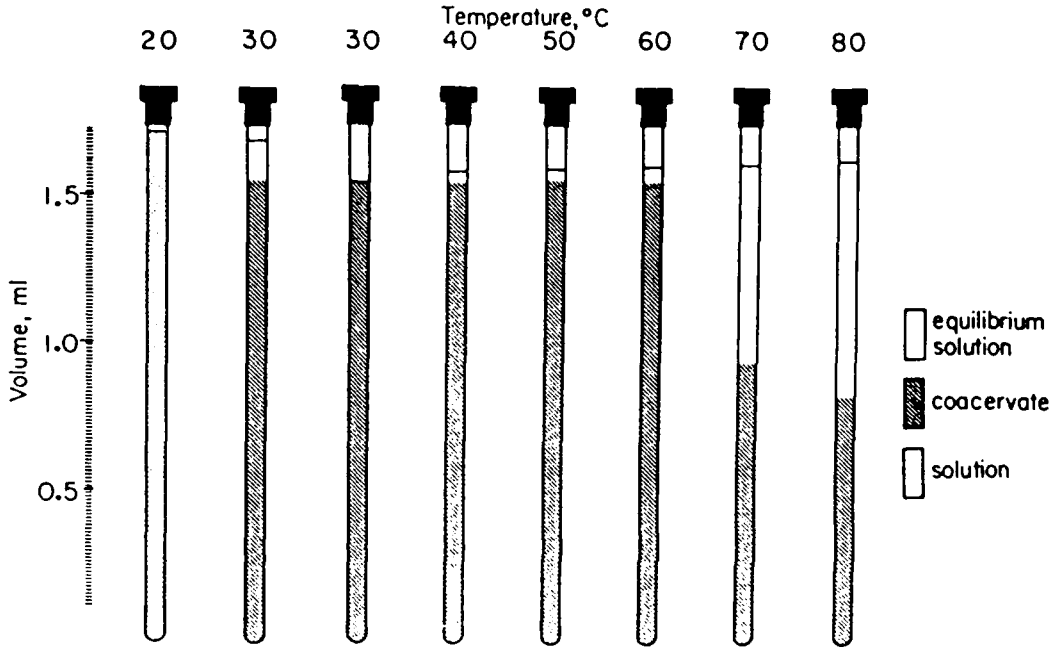

FIGURE 6

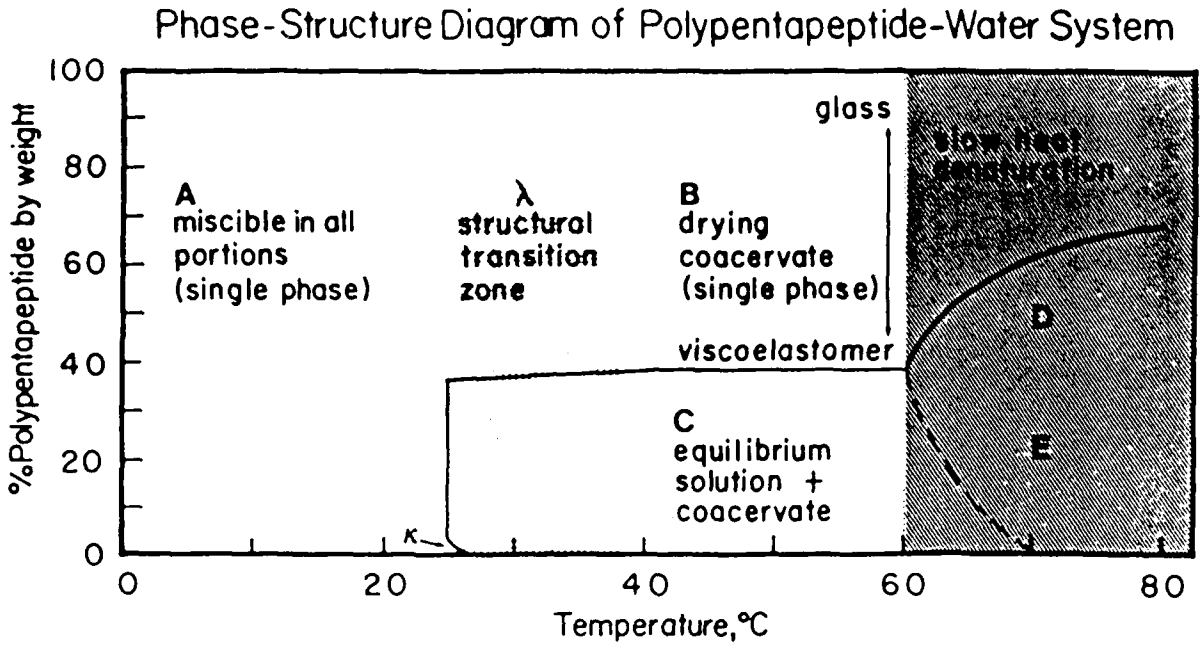
Phase-Structure Diagram of Polypentapeptide-Water System
%Polypentapeptide by weight
100
80
60
40
20
0
0
20
40
60
80
Temperature,°C
A
miscible in all
portions
(single phase)
λ
structural
transition
zone
B
drying
coacervate
(single phase)
glass
viscoelastomer
C
equilibrium
solution +
coacervate
D
E
K

FIGURE 7

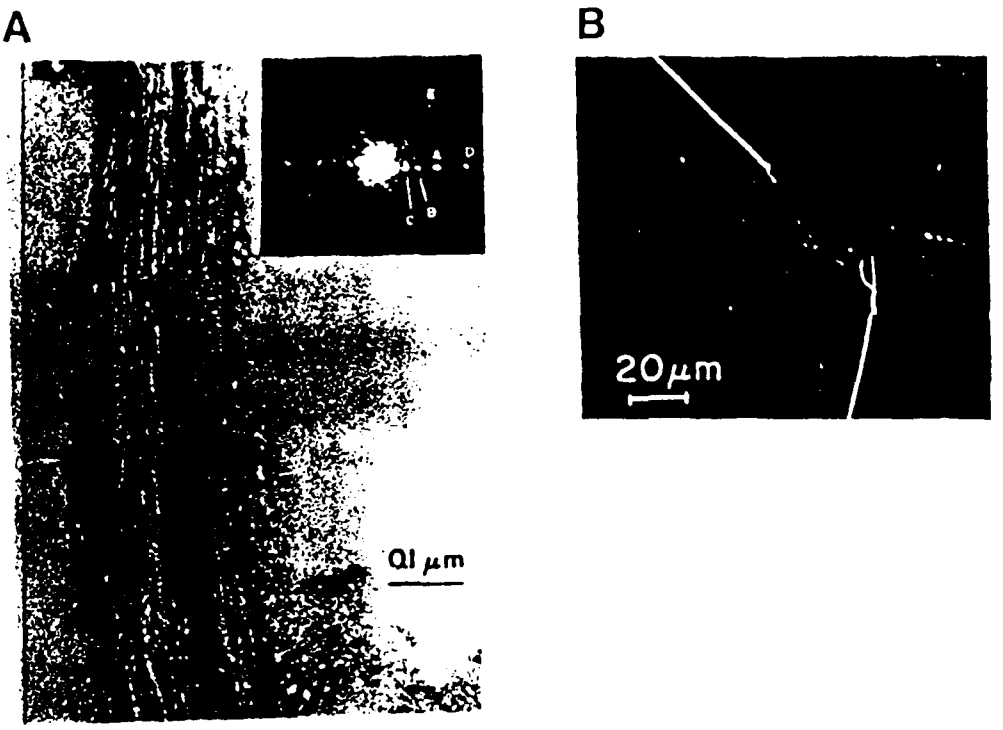

FIGURE 8

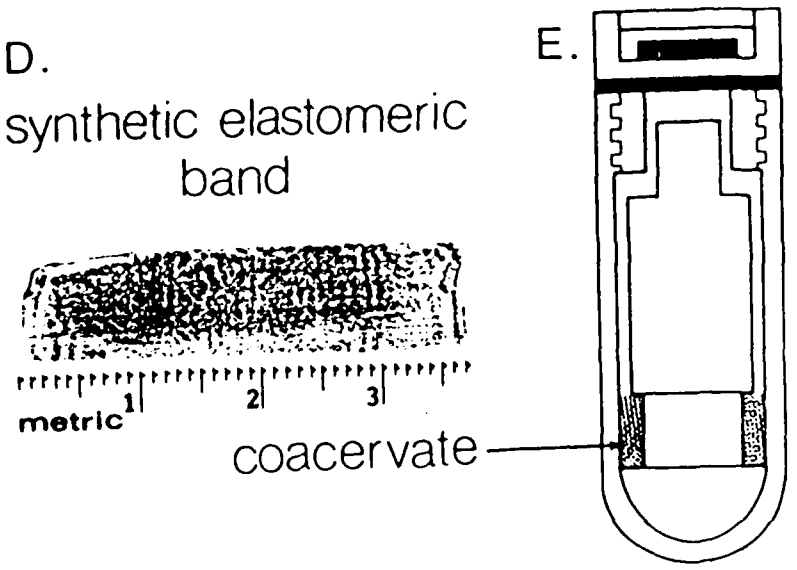

FIGURE 9

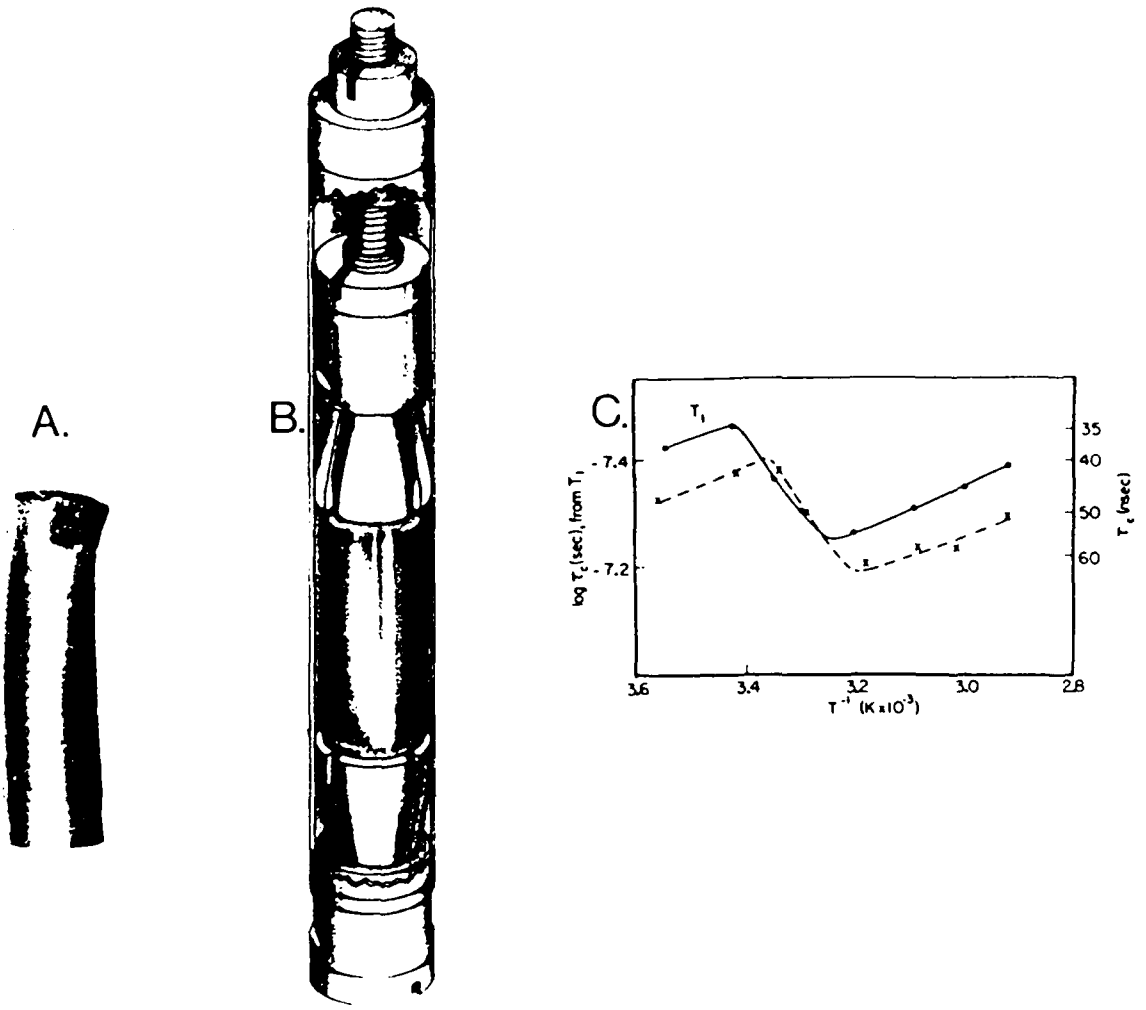
A.
B.
C.
T_1
- 7.4
- 7.2
log T_c (sec), from T_1
35
40
50
60
T_c (sec)
3.6
3.4
3.2
3.0
2.8
T^{-1} (K x 10^{-3})

FIGURE 9

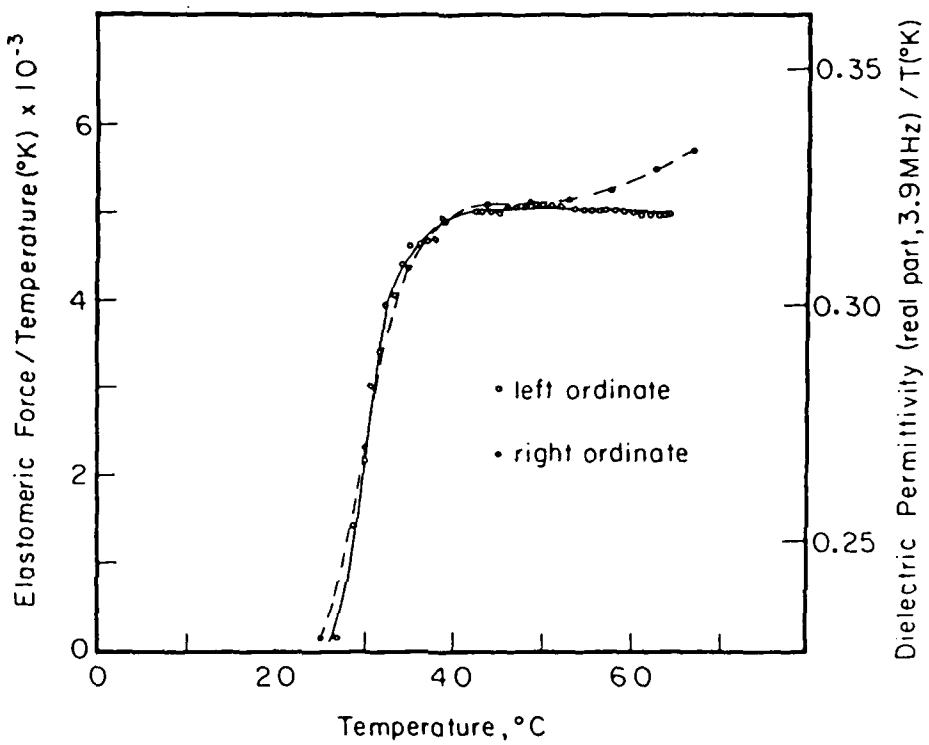
Elastomeric Force / Temperature (°K) x 10^{-3}
Dielectric Permittivity (real part, 3.9MHz) / T(°K)
Temperature, °C
0
2
4
6
0.25
0.30
0.35
0
20
40
60
• left ordinate
• right ordinate

FIGURE 10

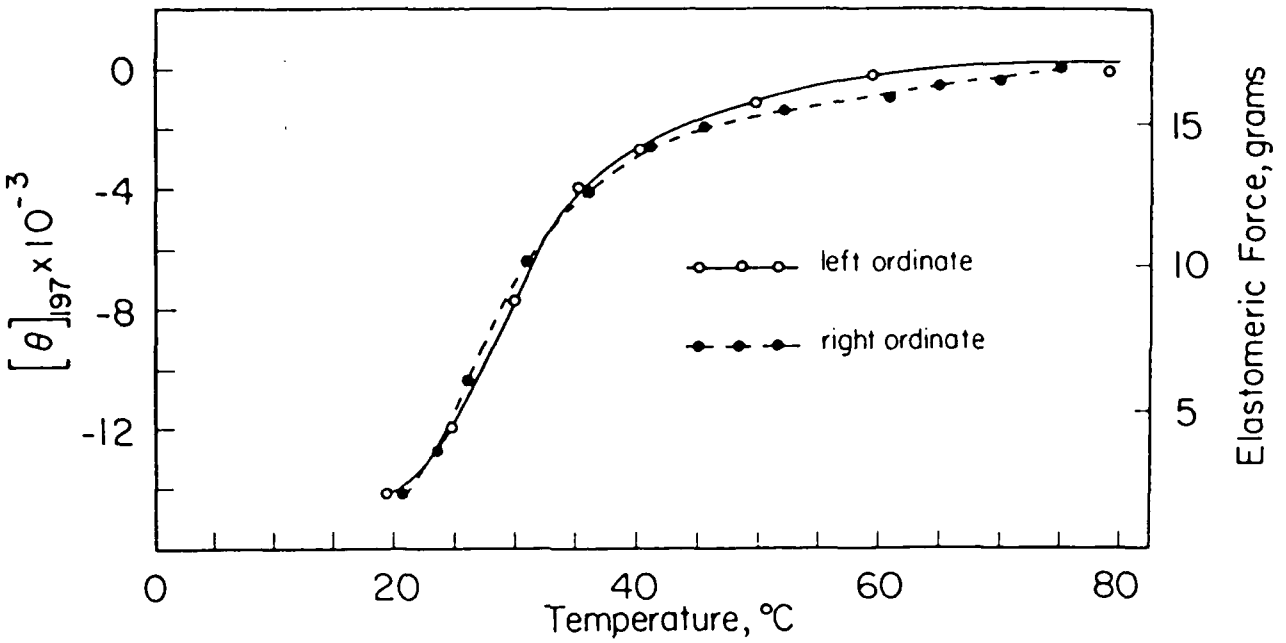
0
-4
-8
-12
$[\theta]_{197} \times 10^{-3}$
15
10
5
Elastomeric Force, grams
left ordinate
right ordinate
0
20
40
60
80
Temperature, °C

FIGURE 11

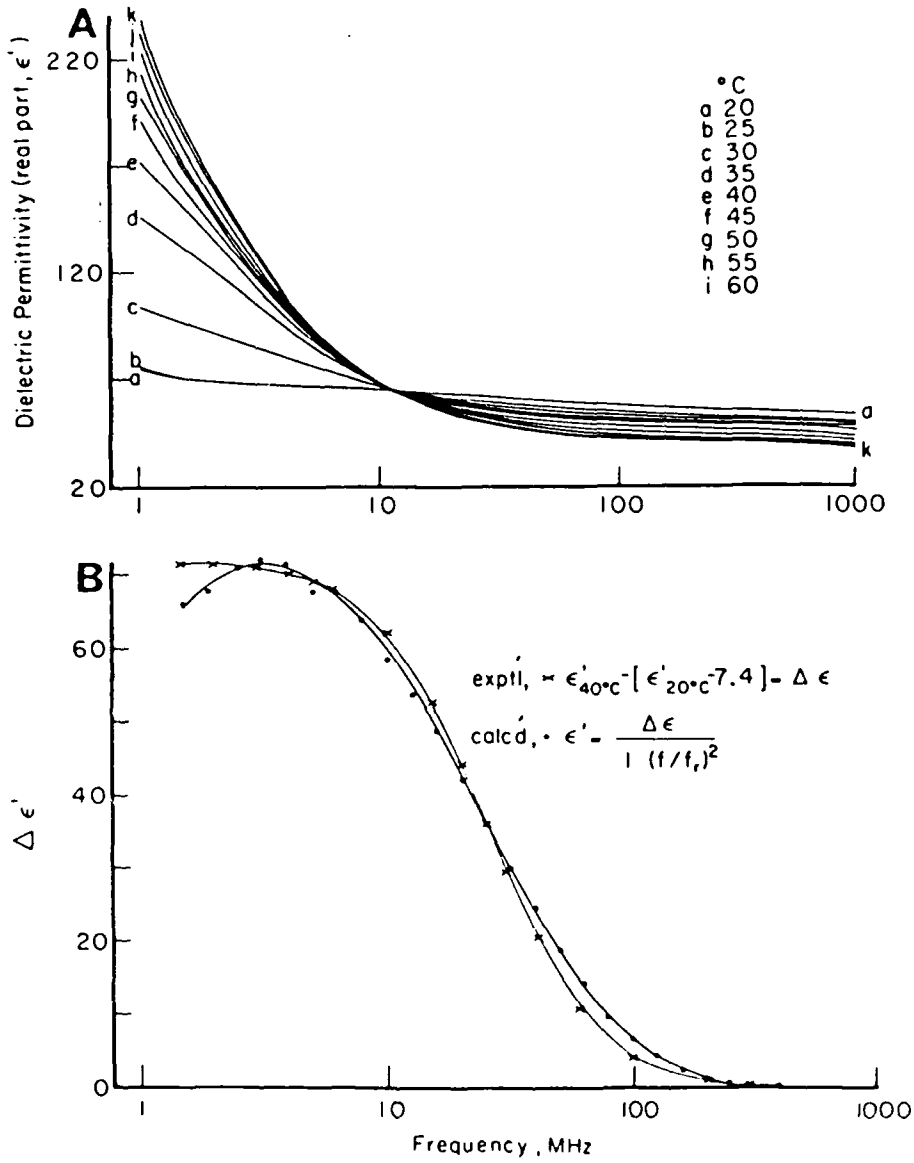
A
Dielectric Permittivity (real part, ε')
220
120
20
1
10
100
1000
°C
a 20
b 25
c 30
d 35
e 40
f 45
g 50
h 55
i 60
B
Δ ε'
60
40
20
0
expt'l, ≈ ε'40°C - [ε'20°C - 7.4] = Δ ε
calc'd, ε' = Δε / 1 + (f/fr)²
Frequency, MHz

FIGURE 12

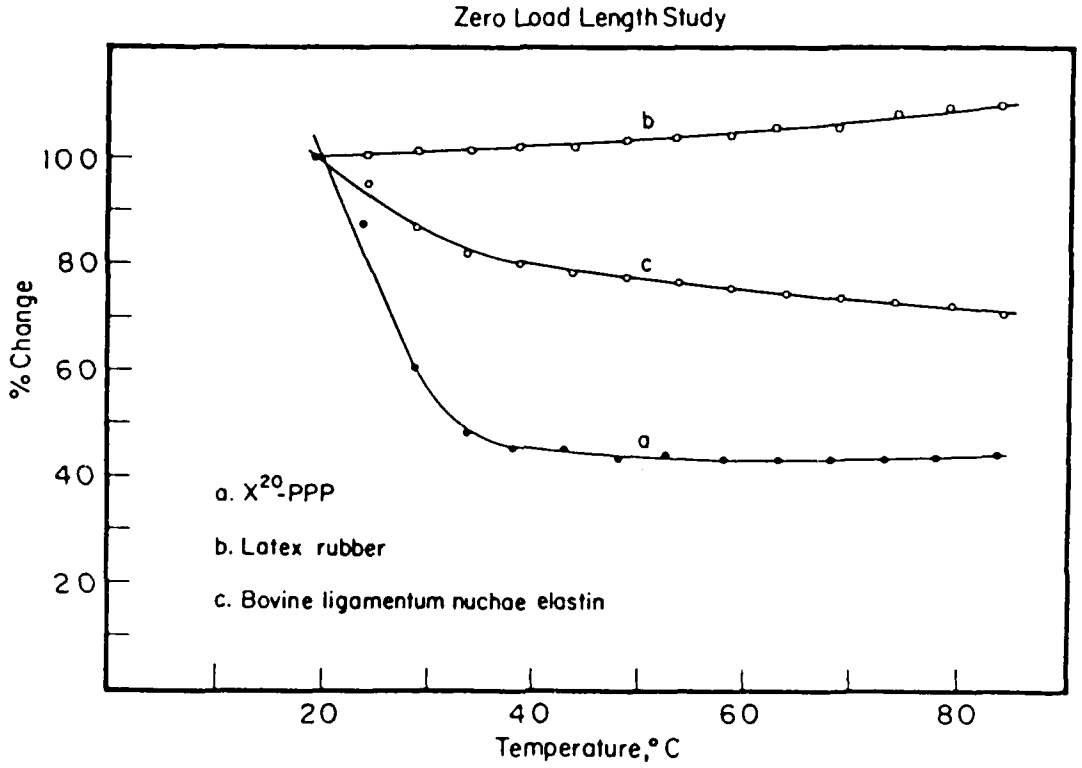
Zero Load Length Study
% Change
100
80
60
40
20
20
40
60
80
Temperature, °C
b
c
a
a. X20-PPP
b. Latex rubber
c. Bovine ligamentum nuchae elastin

FIGURE 13

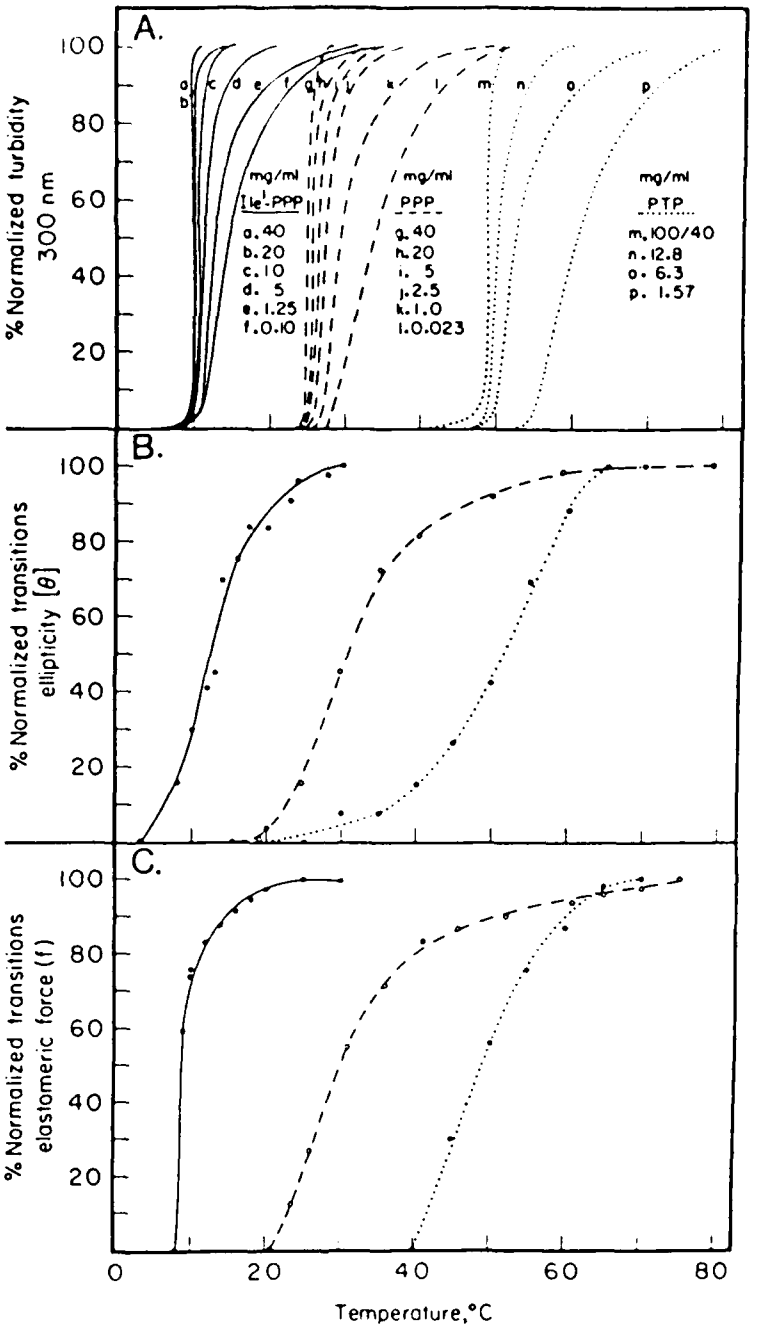
A.
% Normalized turbidity
300 nm
100
80
60
40
20
mg/ml
Ile¹-PPP
a. 40
b. 20
c. 10
d. 5
e. 1.25
f. 0.10
mg/ml
PPP
g. 40
h. 20
i. 5
j. 2.5
k. 1.0
l. 0.023
mg/ml
PTP
m, 100/40
n. 12.8
o. 6.3
p. 1.57
B.
% Normalized transitions
ellipticity [θ]
C.
% Normalized transitions
elastomeric force (f)
0
20
40
60
80
Temperature, °C

FIGURE 14

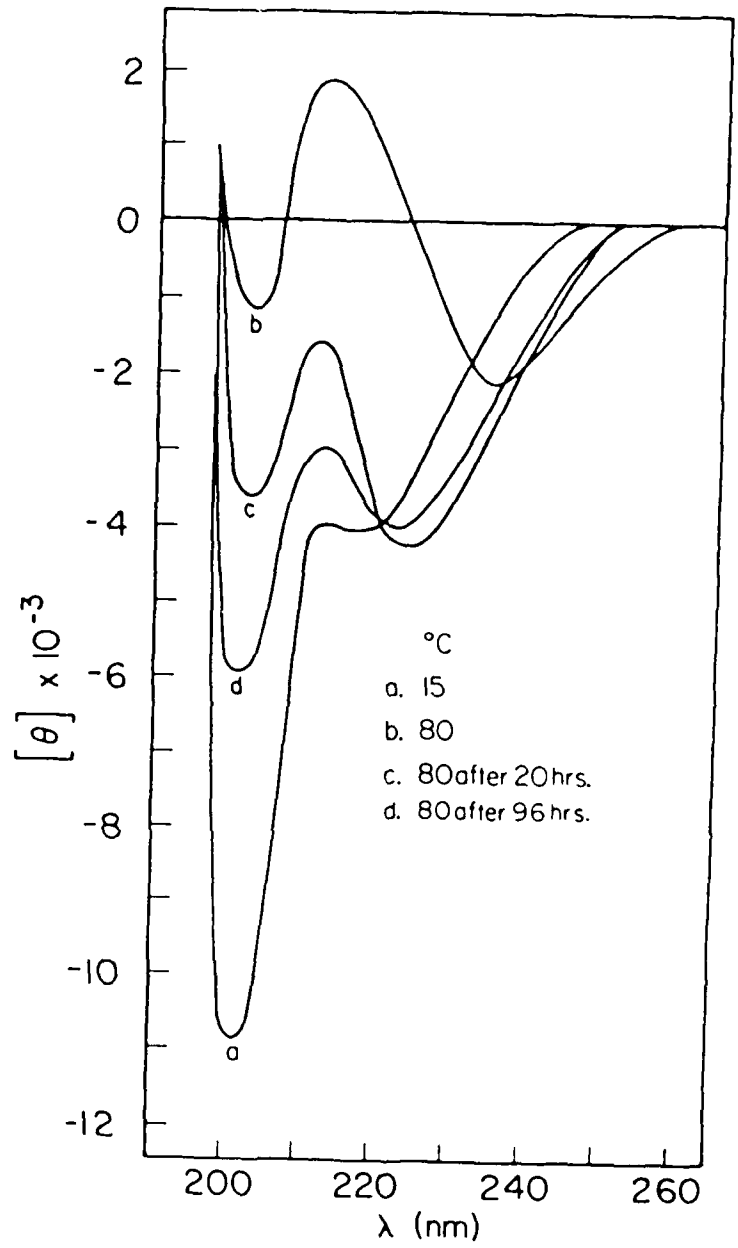
2
0
-2
-4
-6
-8
-10
-12
[θ] x 10^-3
200
220
240
260
λ (nm)
°C
a. 15
b. 80
c. 80 after 20 hrs.
d. 80 after 96 hrs.
a
b
c
d

FIGURE 15

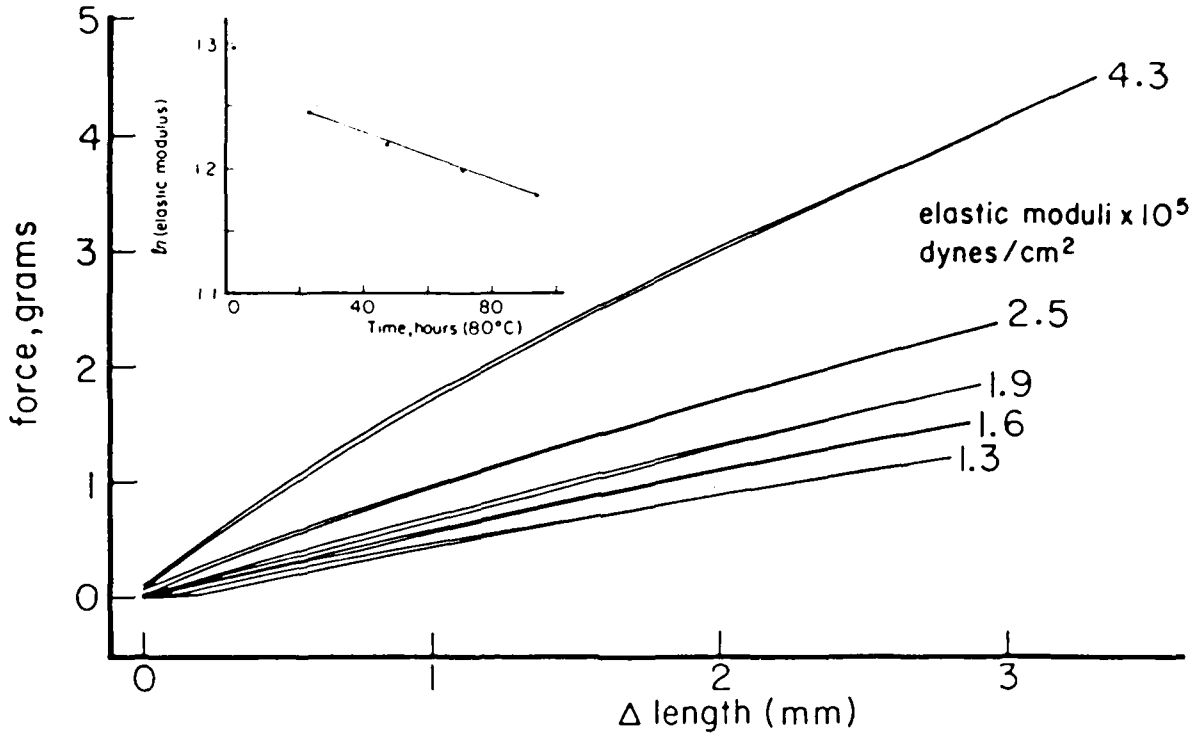
force, grams
Δ length (mm)
elastic moduli x 10⁵
dynes/cm²
4.3
2.5
1.9
1.6
1.3
ln (elastic modulus)
Time, hours (80°C)

FIGURE 16

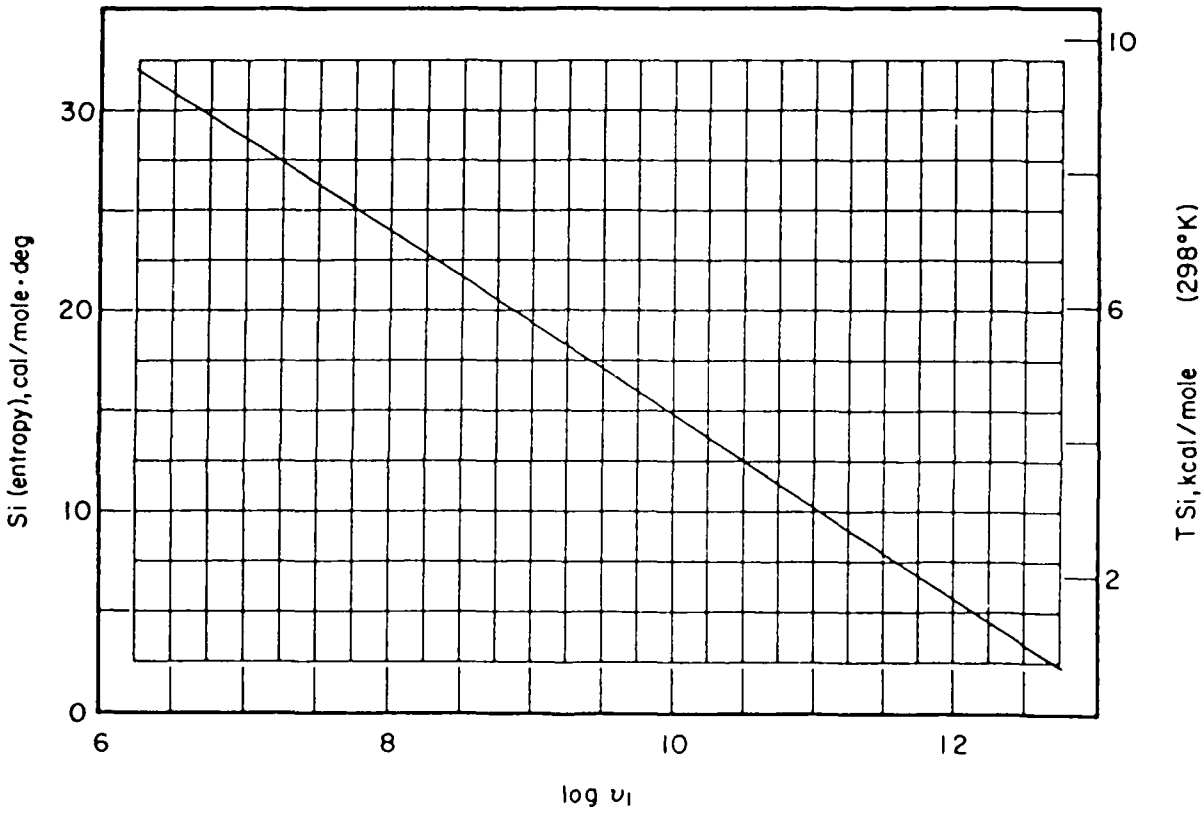
Si (entropy), cal/mole · deg
30
20
10
0
6
8
10
12
log ν_i
10
6
2
T Si, kcal/mole (298°K)

FIGURE 17

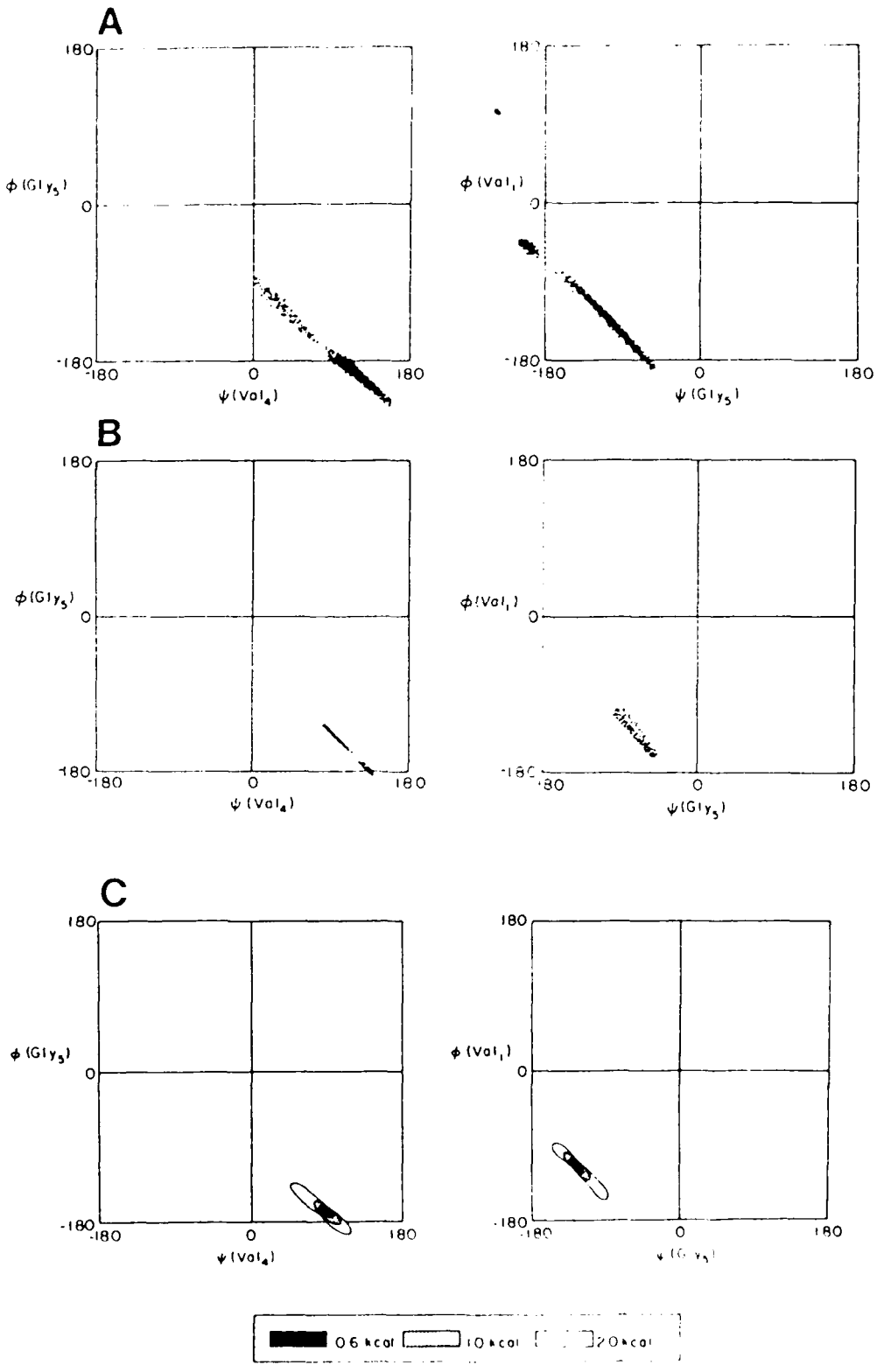
A
B
C
180
0
-180
ϕ (Gly$_5$)
ψ (Val$_4$)
ϕ (Val$_1$)
ψ (Gly$_5$)
0.6 kcal
1.0 kcal
2.0 kcal

FIGURE 18

END

12-87

DTIC